AN INTEGRATED CONTINUOUS MICRO-FLUIDIC SWITCH VALVE

A Thesis Submitted to the

College of Graduate and Postdoctoral Studies

In Partial Fulfillment of the Requirements

For the Degree of Master of Science

In the Department of Mechanical Engineering

University of Saskatchewan

Saskatoon

By

Ashkan Rasouli

PERMISSION TO USE

In presenting this thesis in partial fulfillment of the requirements for a Postgraduate degree from the University of Saskatchewan, I agree that the Libraries of this University may make it freely available for inspection. I further agree that permission for copying of this thesis in any manner, in whole or in part, for scholarly purposes may be granted by the professor or professors who supervised my thesis work or, in their absence, by the Head of the Department or the Dean of the College in which my thesis work was done. It is understood that any copying or publication or use of this thesis or parts thereof for financial gain shall not be allowed without my written permission. It is also understood that due recognition shall be given to me and to the University of Saskatchewan in any scholarly use which may be made of any material in my thesis.

Requests for permission to copy or to make other use of material in this thesis in whole or part should be addressed to:

Head of the Department of Mechanical Engineering

University of Saskatchewan

57 Campus Drive, Saskatoon, Saskatchewan, S7N 5A9, Canada

OR

Dean

College of Graduate and Postdoctoral Studies

University of Saskatchewan

116 Thorvaldson Building, 110 Science Place, Saskatoon, Saskatchewan, S7N 5C9, Canada

ABSTRACT

Traditionally, controllers are an integrated electronic circuit (**IEC**), which is composed of basic modules such as diodes and transistors to provide various logic functions, e.g., switching. The so-called **hard material** refers to materials that have high Young's moduli in comparison with Young's moduli of animal body; otherwise **soft material** is called. The controller built from IEC is called **hard controller** or controller in this thesis. To build a circuit with soft materials, the fluid is naturally taken as a substance, and a circuit can be made by integrating fluid flow and micro-channel deformation. Such a circuit is called integrated micro-fluidic circuit (**IMC**). The controller built from IMC is called **soft controller**.

This thesis was devoted to study IMC, particularly taking the switching valve as a study vehicle. It is noted that the switching valve in IMC corresponds to the diode in IEC. The specific objectives of this thesis are: (1) to develop a new architecture of IMC such that the number of layers of IMC can be reduced to one only, and (2) to build a prototype of the IMC switching valve to explore the feasibility of fabrication of the switch valve based on the proposed architecture in (1).

A comprehensive literature study has resulted in the proposed architecture, which is to "turn" a vertically stacking structure into a horizontally stacking structure. As such, the fluid in the micro-channel horizontally presses the thin wall (or membrane) of the micro-channel to close the micro-channel completely (i.e., the flow is off). Design of a particular switch valve with the help of the axiomatic design theory was carried out. Simulation of the design was carried out by using the multi-physics software COMSOL, which confirmed that if the width of the micro-channel is 13

μm, the membrane with the thickness of 5 μm (length of 140 μm; width of 10 μm) can deflect more than 13 μm, thus closing the micro-channel completely.

The design was then fabricated on the Micro-fabrication facility at Canadian Light Source. Specifically, the material for the switching valve is PDMS owing to its suitable Young's moduli and excellent biocompatibility and the UV lithography together with soft lithography was employed to fabricate the device. Given the capability of the fabrication facility, the membrane with the thickness of 50 microns in the micro-channel was possibly made, which is unfortunate. Due to this reason, a preliminary experiment was performed to observe the deflection of the membrane only, and the result confirmed the expected deflection qualitatively. This limited experiment however helped to verify the simulation system, which thus ensures a certain degree of reliability of the result given by the simulation, namely the complete closure of the channel by the membrane which has the thickness of 5 μm, length of 140 μm, and width of 10 μm. A side finding from this study is that a switching action may not result in 0 (off) or 1 (on) only but x% and y%, where x and y are flow rates and x%+y%=100%. This thesis names such a switch valve continuous switch valve.

The main contributions of the thesis lie in the field of micro-fluidics, and they are: (1) the provision of the proposed architecture of IMC which has one layer in the vertical direction, and (2) the provision of the new concept of switching, namely the continuous switching. The continuous switching may have further implication to information processing, as it departs away from the 0-1 approach, and to actuation, as it exhibits an analogous property as opposed to a digital property.

ACKNOWLEDGEMENTS

After spending one of the best two years of my life at the University of Saskatchewan what I get from this journey is beyond some words. First, a few words will hardly express my sincere appreciation to my research supervisor, Dr. Chris Zhang, for his professional guidance and continuous encouragement throughout my study process. With his continuous guidance and critical comments in my research, I did finish this research which is one of the biggest milestones of my life. I also would like to thank Anthony Tony (a PhD candidate in Professor Zhang's group) for his advice on micro-fabrication as well as simulation of the system. Further acknowledgements are extended to my advisory committee members, Dr. Daniel Chen and Dr. Madan M. Gupta, for their constructive advice and suggestions from the very first AC Committee meeting.

Special thanks go to the Canadian Light Source staffs especially SyLMAND staffs, Mr. Garth Wells and Mr. Michael Jacobs, for their patient guidance and permission to use the facility over there for fabrication of my device. Without their help in the fabrication and their guidance along the path, the goal of this research project could not have been achieved. Besides, special thanks also go to my research group members, especially Mr. Anthony Tony, for his help in all way from start to finish this research and knowledge support.

Finally, I would like to thank my family, especially my wife (Mrs. Fatemeh Zare) and also my parents (Mr. Afshin Rasooli and Mrs. Mehrnaz Banoo Ashraf Ganjouei), for their continuous encouragement, inspiration, and consistent help either mentally, emotionally or finically throughout these years.

TABLE OF CONTENTS

PERMISSION TO USE i

ABSTRACT ii

ACKNOWLEDGEMENTS iv

TABLE OF CONTENTS v

LIST OF FIGURES viii

LIST OF TABLES xiii

Chapter 1 : Introduction 1

1.1 Background and motivation 1

1.2 Research question 5

1.3 Research objective and scope 6

1.4 Organization of the thesis 6

Chapter 2 : Background and Literature Review 8

2.1 Introduction 8

2.2 IEC, IMC, Controller, Hard Controller, Soft Controller 8

2.3 Soft Switch Valve 11

2.4 Alignment in micro-systems 14

2.5 General design methodology 15

2.6 Photolithography and Soft-lithography 17

2.7 Conclusion 19

Chapter 3 : Design of a Novel Soft Switch Valve 20

3.1 Introduction 20

3.2 Design requirement 20

3.3 Conceptual or Concept Design 21

3.4 Embodiment Design and Detail design 25

3.5 Conclusion 26

Chapter 4 : Modeling and Simulation 27

4.1 Introduction 27

4.2 The Schematic Model of the Target System for Simulation 27

4.3 Governing Equation 28

4.4 Model Development with COMSOL 29

4.5 Results and Discussion 32

4.6 Conclusion 40

Chapter 5 : Fabrication and Assembly 42

5.1 Introduction 42

5.2 Fabrication 42

5.3 Assembly 48

5.4 Conclusion 50

Chapter 6 : Experiment 51

6.1 Introduction 51

6.2 Experiment Setup 51

6.3 Results with Discussions 53

6.4 Conclusion 56

Chapter 7: Conclusion and Recommendation 57

7.1 Overview and conclusion 57

7.2 Contribution 59

7.3 Limitations 60

7.4 Future work 60

References 62

Appendix A: Engineering drawings of the prototype system 65

Appendix B: Permission to reproduce Content 70

Appendix C: Calibration and Uncertainty measurement 75

C.1 Uncertainty in measurement 75

C.2 Calibration 76

LIST OF FIGURES

Figure 1.1 the soft controller in the center of Octobot (Wehner et al., 2016).....2

Figure 1.2 The Switch-Valve that is built in three layers (Mosadegh et al., 2010). 5

Figure 2.1 An integrated fluid-mechanical system. 10

Figure 2.2 A switch valve that is built based on the concept of embedded instructions (Mosadegh et al., 2010, 2011). (A) schematics of the normally closed valve (Mosadegh et al., 2011). (B) the main two states of the microfluidic oscillator, as it is stated in the figure, there would be a constant flow that goes directly from each channel and when the pressure builds up in each way, the valve stops the flow of other fluids and goes into the channels itself (Mosadegh et al., 2011). 12

Figure 2.3 Check-valve and Switch valve and their equivalence in the electronic circuit (Mosadegh et al., 2010). In the first column from the left the switch and check valve can be seen in the three layers, the second column shows how the three layers works when fluids go in there. The third column also shows the corresponding symbols of the check valve and switch valve. Finally, fourth column would be the equivalence of the switch and check valve in the electronic circuits.....13

Figure 2.4 The schematic of the fluidic circuit in a fully soft robot (Wehner et al., 2016). It is the controlling system of a soft robot called, Octobot. With this system a fully soft controller has been made and functional for the robot. 14

Figure 2.5 The procedure of Photolithography and soft lithography. (A)-(D) related to fabricating of the micro pattern structure using Photolithography. (E)-(G) would be related to soft lithography process which is using master mold and try to pattern the structure on a PDMS. 19

Figure 3.1 The relationship between the selected FRs and DPs. 22

Figure 3.2. The integration of all the DPs. Z-direction is the gravity direction.....23

Figure 3.3 The function of the new Switch Valve. (a) In this condition, the pressure at the left channel is higher than the pressure at the right channel. Thus, the membrane in the left channel is pushed down while the membrane of the right channel is pushed up and closes the channel of the right channel. In this condition, only the fluid in the left channel can flow; (b) In this condition, however, the pressure of the fluid on the right channel is higher and this leads to the closing of the left channel and consequently the flowing of the left channel stops. 24

Figure 3.4 Embodiment design of the device 26

Figure 4.1 The Schematic Model of the Device: thickness: along Y-axis; width: along Z-axis, length: along X-axis. 28

Figure 4.2 The Geometrical shape for the membrane that have been used. This is for the membrane's thickness of 05µm and the width of 10µm, length of 140µm with the velocity of 1.5m/s. Thickness: along Y-axis; width: along Z-axis, length: along X-axis in reference to Figure 4.1. The fluid geometry is set to 200µm therefore the incompressible fluid can put enough amount of pressure on top of the membrane that can push the membrane further down. The fluid geometry amount can be increased as well but because it makes the rending and data analyzations hard and more time consuming in this study it is set to this amount. 30

Figure 4.3 Meshing of the simulated device. This is for the membrane's thickness of 05µm and the width of 10µm, length of 140µm with the velocity of 1.5m/s. Thickness:

along Y-axis; width: along Z-axis, length: along X-axis in reference to Figure 4.1. 32

Figure 4.4 Comparison of the simulation and experimental results of the vertical deformation of PDMS membrane with its thickness of 50 µm versus different velocities. 33

Figure 4.5 Deflection of the membrane with the membrane's thickness of 05 µm, width of 10 µm, length of 140µm, and the velocity of 1.5 m/s. In this figure the Y axis is the thickness, Z axis is the width, and the X axis is the length of the device in reference to Figure 4.1. All the dimensions in the figure are in microns (µm). 35

Figure 4.6 Deflection of the membrane with its thickness of 05 µm, width of 10 µm, length of 140µm, and the four different velocities. A) deflection of the membrane (2.36 µm) with the velocity of 0.1 m/s; B) deflection of the membrane (7.48 µm) with the velocity of 0.5 m/s; C) deflection of the membrane (11.22 µm) with the velocity of 1m/s; D) deflection of the membrane (14.30 µm) with the velocity of 1.5m/s; the Y axis is the thickness, Z axis is the with, and the X axis is the length of the device; all the dimensions are in microns (µm). 36

Figure 4.7 Vertical deformation of the PDMS membrane with its thickness of 05 µm and different widths and different velocities. 37

Figure 4.8 Vertical deformation of the PDMS membrane with its thickness of 10 µm different widths and different velocities. 38

Figure 4.9 Vertical deformation of the PDMS membrane with its thickness of 50 µm and with different widths, and different velocities. 39

Figure 4.10 Vertical deformation of the PDMS membrane with its thickness of 100 μm, different widths, and different velocities. 40
Figure 5.1 The Laser Machine and the photomask. A. The laser Machine that have been used for making the photomask. B. The photomask which have been created with the laser machine.....43
Figure 5.2 Silicon wafer that is coated with SUEX 44
Figure 5.3 Developer's Bath for the development of the silicon wafer after the post-exposure bake.....45
Figure 5.4 Master mold that has 4 pieces of the device which varies in terms of thickness of the membrane. 46
Figure 5.5 The schematic diagram of the device which has two channels and the membrane is the space between two channels the fluid goes on the top channels and put pressure on the membrane and try to push the membrane down. 47
Figure 5.6 there are four different PDMS molds that has been getting from the silicon wafer and ready for the bonding to the glass. 48
Figure 5.7 The oxygen plasma that has been used for bonding the PDMS to the glasses.49
Figure 5.8 two of the PDMS membranes which have been bonded to the microscopic glasses. 50
Figure 6.1 Instruments used in the experiment. (a) micro-lens, (b) syringe, (c) needle. ...52
Figure 6.2 A sample of one of the membranes with the size of 50 μm in thickness of the membrane.....53
Figure 6.3 injection of the colored water into the main channel by using the needle. 54

Figure 6.4 The examination of using a 30G needle and colored fluid. In the pictures above by injection of the fluid inside the main channel, small deformation of the membrane can be observed. From the A-F, the small deformation of the membrane can be seen. (A) the colored water is injected and all of the top and the bottom channels of the membrane are filled with the colored water. (B, C) with the help of the needles all of the areas which has small air inside will be taken away and filled with water instead. (D) a pressure is increased with the help of the needle and by inserting more colored water. Therefore, small amount of movement is observed where a membrane touches the other channel. (E, F) The movement continues as the pressure was increased by the needles. 55

Figure A.1 The exact Dimension of the Switch Valve in micron (µm).....66

Figure A.2 The proposed design of the Switch Valve on top of a Silicon Wafer 67

Figure A.3 Four membranes in one Silicon Wafer.....68

Figure A.4 The exact Dimension of one of Membrane with the thickness of 50µm.....69

Figure C.1 Multifunction target calibrator (Model DA030). It has a precise measurement which can be viewed under the microscope and with that precise measurements the calibration can be done. 76

Figure C.2 The measurements which have been done by using a microscope.....77

Figure C.3 Microscope which used for capturing some of the images and also measure the calibration 77

LIST OF TABLES

Table 4.1 The amount of deformation between Simulation and Experimental results for the membrane with the thickness of 50μm, the length of 140μm, and the height of 25μm. 34

Chapter 1 : Introduction

1.1 Background and motivation

Nowadays, most of the controllers that are built using electronic devices such as transistors and diodes. These devices are essentially electronic circuits, which are made of the “hard” materials such as silicon-based materials. Controllers or control systems are essentially an integrated electronic circuits (IEC), and they are thus called hard controller in brief. A more elaboration on IEC and hard controller can be found in Chapter 2 of this thesis.

In some cases, the controllers built from the “soft” materials are needed or desired in devices used inside the human body (particularly near the important organs such as the heart). Such controllers are called **soft controller** in brief. Figure 1.1 shows a so-called fully unthreatened soft robot (Octobot), in which a great attention lies in its control system which is made by a soft controller. To build a soft controller, the fluid is taken as a substance together with the microfluidic or channel device, which is made from the soft materials. A more discussion of soft controller can be found in Chapter 2.

In this thesis, the definition of soft materials follows the one in (Rus & Tolley, 2015) , i.e., soft materials are those materials with their Young’s moduli being compatible with those of the animal body. In our group (Chen et al., 2017), materials are viewed as a system, so the environment makes sense. Then, a new concept called “**relative softness”** for a material system was introduced, details

of which refer to (Chen et al., 2017). Thus thesis takes the definition of (Rus & Tolley, 2015) owing to its practicality and simplicity to the work presented in this thesis.

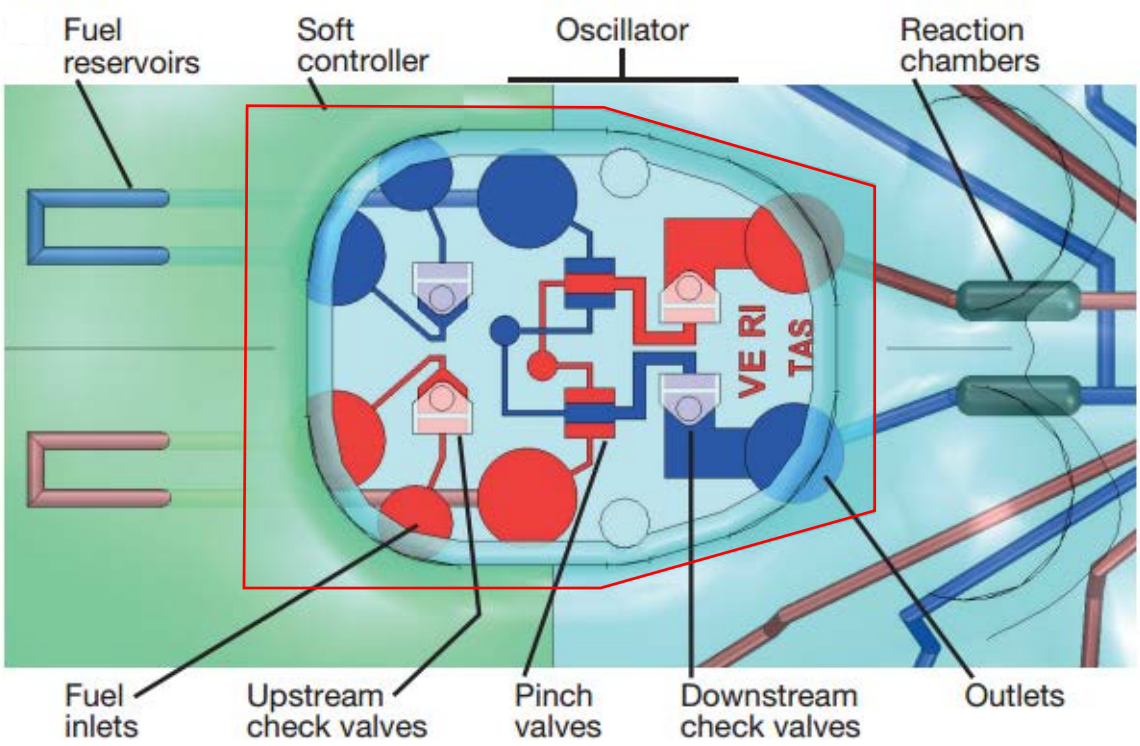

Figure 1.1 the soft controller in the center of Octobot (Wehner et al., 2016).

It can be anticipated that the behavior or more precisely speaking, the logic behavior of a soft controller depends on the fluid and its handling microfluidic device, two of which are highly integrated and follow the system architecture called "**instance-infrastructure (I-S)**" (Zhang & van Luttervelt, 2011; Zhang and Wang, 2016). Since a controller is essentially a logic circuit, the soft controller is essentially an integrated microfluidic circuit (**IMC**). Hereafter, soft controller and IMC are used interchangeable, and more discussions on IMC and soft controller can be found in Chapter 2.

The traditional electric controllers or hard controllers have several basic modules such as diodes and transistors. To soft controllers, therefore a need to develop the IMC modules that can behave the similar functions as those IEC modules arises.

Over the past ten years, there is a great effort in building IMC modules as well as the whole control system with the feedback feature (Wehner et al., 2016; Kruse et al., 2011); see Figure 1.1. One challenge with IMC is to realize the feedback control, which is also called **self-control** or **embedded instruction** in the context of IMC. By self-control it is meant that an IMC system can perform feedback control without any external electronic element (Mosadegh, Bersano-Begey, Park, Burns, & Takayama, 2011). A more discussion on embedded instruction can be found in Chapter 2.

One of the first designs of an IMC system with embedded instructions to demonstrate how the self-control concept works is a normally-closed valve (i.e. the valve that is closed in a normal condition and would be open by receiving a signal from controller), which performs self-switching (or switching without any electronic element or self-control) of the outlet flow between two flows (Mosadegh et al., 2010). According to (Mosadegh et al., 2011), the concept of the switching valve in IMC is not new; see the work of (Groisman, 2003; Henning, 2007; Jeon et al., 2002; Kartalov, Walker, Taylor, Anderson, & Scherer, 2006; Langelier, Chang, Zeitoun, & Burns, 2009; Liu, Chen, Taylor, Scherer, & Kartalov, 2009); however, the switching based on the self-control concept (or self-switching) is new. The concept of self-control in the context of fluid systems based on the I-S architecture is, in short, that the control decision is embedded in the fluid system. Details of the self-control concept will be discussed in Chapter 2.

The self-switching valve developed by (Mosadegh et al., 2010) is shown in Figure 1.2. As it is shown in Figure 1.2, the switching valve was built with three layers, inside which the fluid flows. Two fluids (A and B) flow within the system with one (A) on the upper part of the membrane and the other (B) on the lower part the membrane. By manipulating the pressure of A and B, one can make the membrane deforms upward and downward (Figure 1.2). When the membrane deforms upward, the flow of A stops while B flows, and when the membrane deforms downward, the flow of B stops while A flows. In this way, a kind of switch valve is realized. Feedback can be further realized by another system that closes the loop to form an application system, e.g., oscillator with embedded instruction (or without external electronic systems) involved (Mosadegh et al., 2010).

In fact, the principle of the embedded instruction system is coupling of fluid dynamics and channel or membrane elasticity. The design challenge is to represent and realize the circuitry behavior and control behavior with the integrated **flow-deformation** system, such as check valve for diode and switch valve for transistor.

A preliminary study of the system of Figure 1.2 reveals that it has two potential limitations. The first limitation is that the three-layer system is difficult to make at the micro scale level, the difficulty to fabricate and also to bond them. For example, just for the simple bonding using oxygen plasma, according to (Mosadegh et al., 2010), they did it in three steps (hold the membrane's flexibility and put the appropriate holes into the device, so only aligned the three layers by aligning the holes. The second limitation is that the device cannot achieve a switching function to the amount of the flow rate in such a way that x%+y% = 100%, where x, y is the flow rate; instead, it

only achieves a switching function or either x=0 and y=100 or x=100 and y=0. This thesis was motivated to address these two limitations.

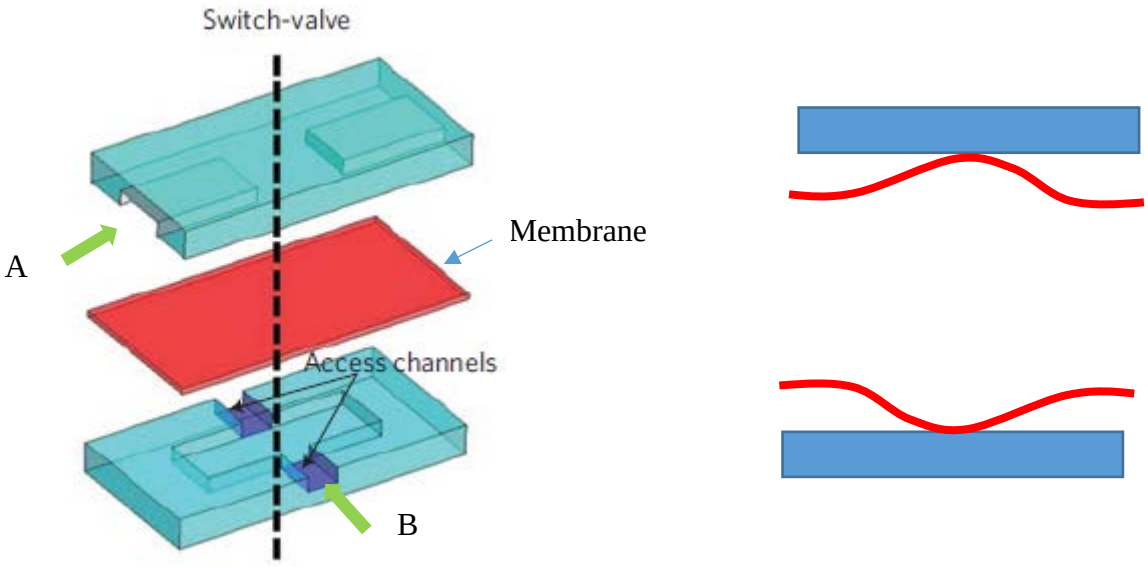

Figure 1.2 The Switch-Valve that is built in three layers (Mosadegh et al., 2010).

1.2 Research question

Can we have a new architecture of the flow-deformation system such that the switch valve can be realized by reducing the number of layers in the system of (Mosadegh et al., 2010) and if this is possible what will be pros and cons of the new architecture with respect to the three-layer architecture?

1.3 Research objective and scope

The **overall objective** is to develop a new architecture for the flow-deformation system such that the switch valve with the embedded instruction can be built. It is noted that this thesis does not attempt to develop any application system upon the switch valve at the point of time this research was carried out. To achieve the overall objective, the following specific objectives were proposed.

- ***Objective 1****: To investigate the new architecture of a micro-fluidic device that reduces the number of layers of flow-deformation systems for performing the function of switch valve.*
- ***Objective 2:*** *To develop an accurate simulation model for a flow-deformation system which is built upon the new architecture to predict the behavior of the system.*
- ***Objective 3****: To build a prototype for the foregoing flow-deformation system to prove that the proposed architecture works.*

1.4 Organization of the thesis

The remaining part of this thesis is organized as follows. Chapter 2 will provide further background information and discussion of related work pertinent to the proposed research objectives. In Chapter 3, a new architecture of the flow-deformation system for switch valve will be presented along with design of a flow-deformation switch valve system based on the new architecture. Chapter 4 presents the mathematical model of the switch valve to predict its behavior to give confidence for prototyping of the switch valve. Chapter 5 discusses the fabrication and assembly of the device. Chapter 6 discusses the experiment on the prototype of the switch valve. Finally,

Chapter 7 presents conclusions, contributions, and limitations of the work as well as some thoughts for further research.

Chapter 2 : Background and Literature Review

2.1 Introduction

This chapter will discuss some background information in detail and critically comment on related work. In Section 2.2, the concept of IEC, IMC and soft controller will be further discussed. Section 2.3 will discuss self-switching valve or soft switch valve and its application in IMC and soft controller. Section 2.4 discusses the alignment technique for micro-systems to highlight the challenge with the technique. Section 2.5 discussed systematic design methodology. Finally, there is a discussion of the need of the proposed objectives in Chapter 1.

2.2 IEC, IMC, Controller, Hard Controller, Soft Controller

According to (Tu et al., 2008), control is a process to adjust the input to a system based on the performance of the system, and the control process is accomplished by a system called controller. For a controller to work, there is a need of the sensor which can understand the performance of the system. The controller decides on an action, and that action will further be taken to realize the adjustment to the input to the system. By the way, the concept of control was extended to management by (Wang, Wang, Zhang, Ip, & Furuta, 2014), that is, control is part of a much broader activity to manage operation. This thesis focuses the narrow definition of control.

In the early time, the controller, sensor and actuator were all performed by the mechanical system (Figure 2.1). In Figure 2.1, once the pressure in the vessel is over a certain value, the bar will be

up to open the valve, so the gas in the vessel is released to outside, and this then brings the pressure in the vessel down. By incorporating electronics into the system, the pressure in the vessel may be measured by the electronics-based sensor. The controller will be implemented by a computer system which is represented by software (e.g., if the actual pressure is larger than 50 psi, then to actuate the bar up to open the valve). The software can be represented by the physical circuit. As such, one can imagine the whole system is an integration of the mechanical components and electronics components, and there are mechanical movement and electronic charge movement. This system is called integrated electronic circuit (IEC).

The equipment that handles the charge is based on the materials with a very high melting point (e.g., silicon). The Young's moduli of such materials are far higher than those of animals. Such an IEC is called hard IEC, and correspondingly, the controller built from the hard IEC is called hard controller. Note that the definitions of hard IEC and hard controller are not seen in the literature.

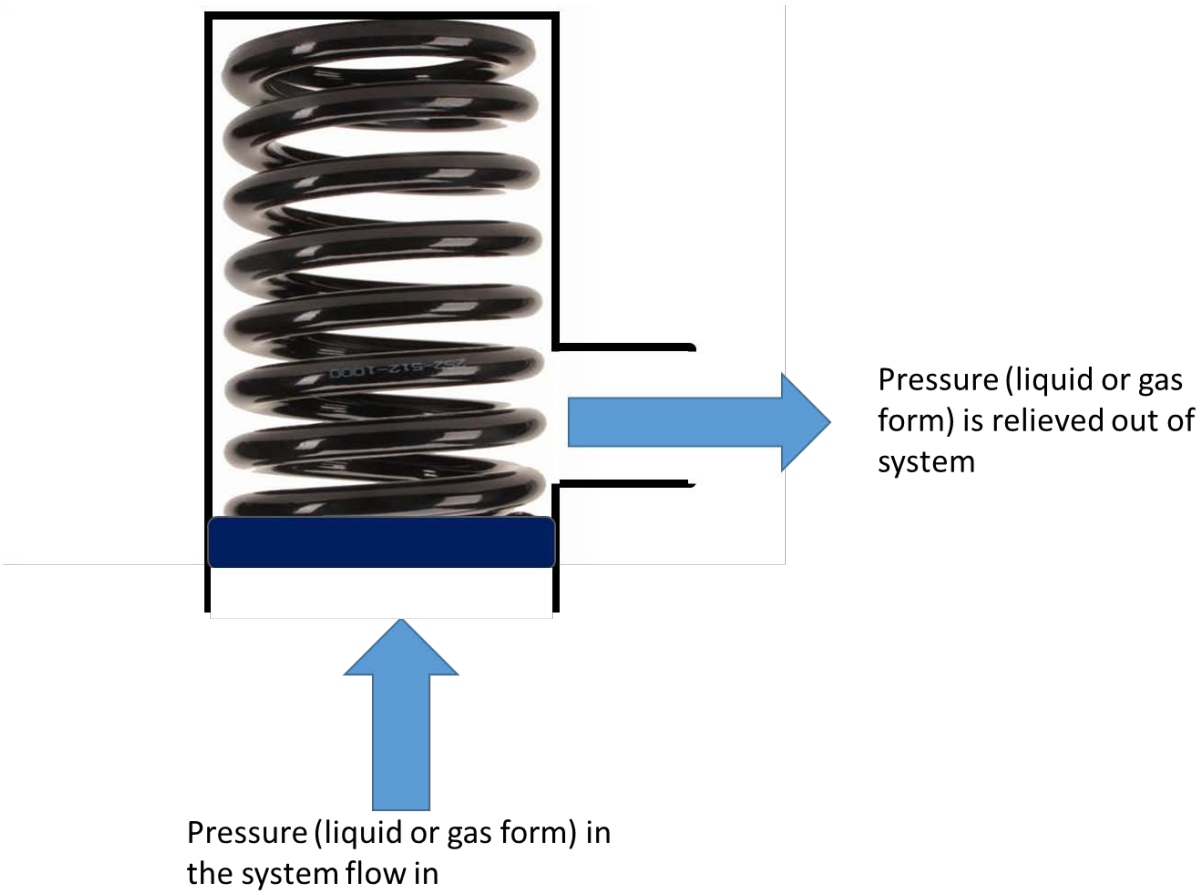

Figure 2.1 An integrated fluid-mechanical system.

When the electronic charge is replaced by the fluid, the whole system, as described before for the charge and mechanical system, is an integrated micro-fluidic circuit (IMC). In fact, more precisely, such a system should be called integrated fluid circuit, but this thesis still uses the term of IMC for consistency with the literature. When the Young's moduli of the materials that handle fluid are compatible with those of animals, the IMC is called **soft IMC**. Correspondingly, the controller built from the soft IMC is called **soft controller**.

The controller uses control knowledge (e.g., ‘if the pressure in the vessel is greater than 50 psi, the gas in the vessel lifts the valve and by pass from the exit A’) to perform its decision-making function, and each controller has its own control knowledge base. The control knowledge base may be embedded inside the controller or may be delegated to an outside source. For instance, the control knowledge base in Figure 2.1 is embedded inside the controller. Since the control knowledge is an instruction for action, the embedded control knowledge is also called imbedded instruction in literature (Mosadegh et al., 2010; Mosadegh et al., 2011). The controller with imbedded instruction is also called self-controller. The IEC based controller usually has embedded instruction, so it is a self-controller or just controller otherwise stating explicitly that the knowledge base is from an external source. The soft IMC based controller with embedded instruction is called soft self-controller.

It is noted that the concept of embedded instruction was introduced from soft IMC in literature (Mosadegh et al., 2010; Mosadegh et al., 2011), which is not as broad as the one introduced in this thesis. There have been some developments on soft IMC with embedded instruction, or soft IMC controller, e.g. the work of (Mosadegh et al., 2011) for a soft self-control system for oscillator (Figure 2.2) and the work of (Wehner et al., 2016) for a soft robot. These developments are far less systematic that the developments on IECs.

2.3 Soft Switch Valve

Switch valve is essentially for changing the direction of the flow (Mosadegh et al., 2010). In the case of IEC devices, a switch valve changes the direction of the electric current in circuit. In the

case of IMC devices, a switch valve changes the direction of flow of the fluid in circuit. In IEC or electric circuit, the transistor p-channel Junction Field Effect Transistor (JFET) (Mosadegh et al., 2010) serves to change the flow direction of the charge.

Diode and transistor are two basic components in electric circuits. Diode plays a function that the charge can only flow in one direction but not opposite direction (Mosadegh et al., 2010). Transistor plays a function of controlling the charge in the circuit by direct the voltage into different direction (Mosadegh et al., 2010). Figure 2.2, shows the possible scheme of IMC to mimic diode and transistor.

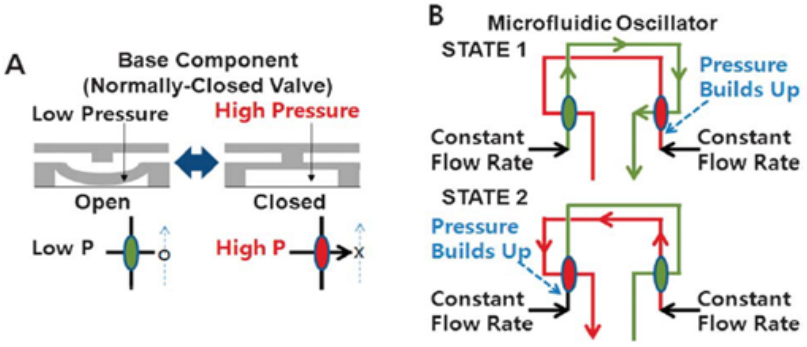

Figure 2.2 A switch valve that is built based on the concept of embedded instructions (Mosadegh et al., 2010, 2011). (A) schematics of the normally closed valve (Mosadegh et al., 2011). (B) the main two states of the microfluidic oscillator, as it is stated in the figure, there would be a constant flow that goes directly from each channel and when the pressure builds up in each way, the valve stops the flow of other fluids and goes into the channels itself (Mosadegh et al., 2011).

Only a few studies on the IMC device to mimic the function of diode and transistor. The check valve (for mimicking diode) and switch valve (for mimicking transistor), along with an oscillator were developed by (Mosadegh et al., 2010) – see Figure 2.2. This system was further applied to a

fully soft robot by (Wehner et al., 2016) – see Figure 2.2. The basic building block for the IMC system developed by (Mosadegh et al., 2010) is a three-layer architecture (Figure 1.1). The three-layer structure creates two chambers of fluid, upper fluid (A) and bottom fluid (B), between which is a membrane that deflects to stop the flow A but to start the flow B alternately. The limitation of this architecture is the difficulty in assembly of the three components in a good alignment.

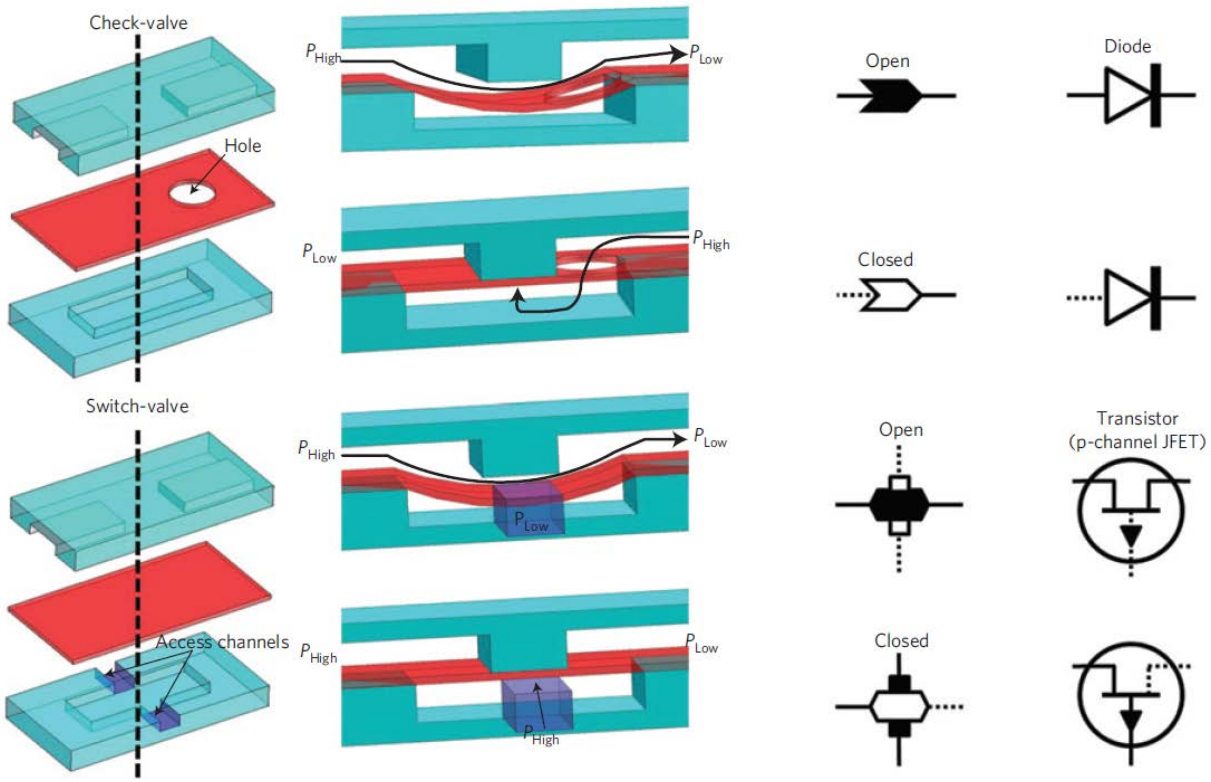

Figure 2.3 Check-valve and Switch valve and their equivalence in the electronic circuit (Mosadegh et al., 2010). In the first column from the left the switch and check valve can be seen in the three layers, the second column shows how the three layers works when fluids go in there. The third column also shows the corresponding symbols of the check valve and switch valve. Finally, fourth column would be the equivalence of the switch and check valve in the electronic circuits.

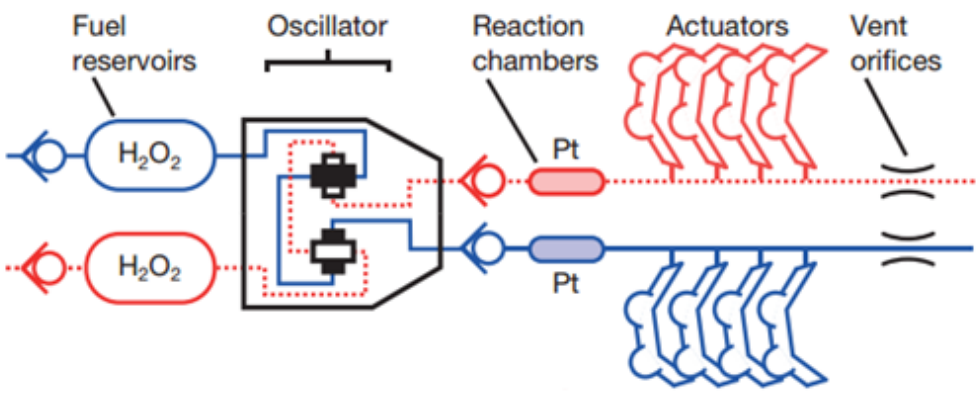

Figure 2.4 The schematic of the fluidic circuit in a fully soft robot (Wehner et al., 2016). It is the controlling system of a soft robot called, Octobot. With this system a fully soft controller has been made and functional for the robot.

In this thesis, an extension to the switch valve was found interesting, that is, the switch is not only performed in a 0-1 manner but also performed in proportion in terms of flow rate between A and B. For instance, the switching may take places between 25% of A and 75% of B. The system made by *Mosadegh et al. (2010*) cannot achieve this kind of switching.

2.4 Alignment in micro-systems

The fabrication of the IMC is a cumbersome process that needs dedication and precision. In this case, the layers make the fabrication process much more difficult. One challenge is that the bonding process must be completed within a couple of seconds after fabrication of the upper and bottom parts because the oxygen plasma boding procedure requires. According to (Mosadegh et al., 2010), a three-step pre-assembly process needs to be done before the alignment process can be

proceeded. Another issue with the multi-layer assembly system is leakage. Obviously, the more layers, the more leakage.

2.5 General design methodology

In this section, design theory and methodology applied to designing the novel soft self-switch valve is introduced. Design of a system is divided into four phases:

- Development of design specification.
- Concept or conceptual design,
- Embodiment design,
- Detail design.

Design specification refers to the information about the customer requirement, which is described in technical terminology (Zhang, 2017). Concept design refers to the determination of the principle of a device that can fulfill the required function under the required constraint. Embodiment design refers to materializing and configuring materials to the device that is based on the principle. Detail design refers to a complete specification for each individual component ready for manufacturing.

The requirement is divided into the function requirement (**FR**) and constraint requirement (**CR**). In FR, the performance requirement (**PR**) is also specified, which means how well a FR is performed. FR means functions that a device must achieve, and CR means the condition where a device achieves its FR. A design refers to a structure that is able to fulfill FR and CR. The design specification contains both FRs and CRs.

The description of the structure is via parameter, which is also called design parameter (**DP**). DP may not correspond to a specific dimension, e.g., diameter of a cylinder, and DP is in essence a description of design. At the concept design phase, DP thus describes the concept upon which the embodiment and detail information about a device is further created.

To a complex design, the overall FR may need to be decomposed, say FR is decomposed into FR 1 and FR 2 (Pahl et al., 2013). Accordingly, DP follows the decomposition, that is, DP is decomposed into DP 1 and DP 2, where DP 1 fulfills FR 1 and DP 2 fulfills FR 2. It is noted that the foregoing decomposition makes sense to concept design only. In fact, according to the definition of embodiment design and detail design, both refers to determining the material, volume, and surface feature of a device to further achieve PR and CR.

There are three types of relationships between FRs and DPs, which are described by Equation 2.1, 2.2, and 2.3:

$$\begin{bmatrix} FR1 \\ FR2 \end{bmatrix} = \begin{bmatrix} A11 & \\ & A22 \end{bmatrix} \begin{bmatrix} DP1 \\ DP2 \end{bmatrix} \quad \text{Uncoupled} \tag{2.1}$$

(Diagonal matrix)

$$\begin{bmatrix} FR1 \\ FR2 \end{bmatrix} = \begin{bmatrix} A11 & \\ A21 & A22 \end{bmatrix} \begin{bmatrix} DP1 \\ DP2 \end{bmatrix} \quad \text{Decoupled} \tag{2.2}$$

(Triangular matrix)

$$\begin{bmatrix} FR1 \\ FR2 \end{bmatrix} = \begin{bmatrix} A11 & A12 \\ A21 & A22 \end{bmatrix} \begin{bmatrix} DP1 \\ DP2 \end{bmatrix} \quad \text{Coupled} \tag{2.3}$$

(Full matrix)

A very important theory to guide the function decomposition and for determining DP is Axiomatic Design Theory (ADT), developed at MIT (Suh, 1990; Suh, 2001). ADT is further revised by Fan et al. (2015) to clarify some concepts in (Suh, 1990). Axiom 1 was found very useful to the present study. Axiom I is stated as follows:

Axiom 1 (The Independence Axiom):

(1) Design or function requirements (FR) should be independent or uncoupled on their own right.

(2) Design parameters (DP) should maintain the FRs independent or uncoupled (including decoupled).

Remark 2.1: Axiom 1 suggests a better design to be uncoupled or decoupled. It is applicable to concept design.

Remark 2.2: Concept design is also called logical design, which emphasis a sense of non-physics. Therefore, the independency of designs (DP-FR relation) does not mean that physically, each DP is a physically separate piece.

2.6 Photolithography and Soft-lithography

Fig. 2.5 illustrates an important fabrication technique for a Micro-Electro-Mechanical Systems (MEMS) or a micro-system which has its overall size less than 100 μm. In Fig. 2.5, the energy beam is UV light (but can be other types of energy beam). The process starts with a wafer which

is usually made of silicon material (Si) (Fig. 2.5A), and the goal is to produce the MEMS of Fig. 2.5G. Coat a photo-resistive material (or photo-resist) on the top of Si (Fig. 2.5B). There are two types of photo-resists: positive and negative; they are chosen based on the final product. In Fig. 2.5, a negative photo-resist called SU-8 is chosen. The photo-resist is usually spin-coated with a specific speed to achieve a uniform coating on the Si wafer. The coated substrate is then placed under the UV light for exposure covered by a photomask which needs to be made beforehand. The photomask has the pattern of the design. After the exposure, the silicon wafer is ready for development, and at this stage, most of the pattern and design can be seen with unarmed eyes and can be also seen underneath of a microscope. Fig. 2.5D is a mold, at which the conventional photo-lithography approach ends. Soft lithography goes on from here (Fig. 2.5D), particularly, the mold in Fig. 2.5D is taken to make parts with any other type of material, e.g., PDMS. Fig. 2.5E shows how the PDMS material is put on the mold, and then the PDMS is peeled off from the mold to form a channel structure (Fig. 2.5F). Finally, The PDMS bond to a glass with various method like oxygen plasma (Fig. 2.5G). It is noted that the PDMS product can be used as a mold by itself to make another patterned part with materials that have lower melting points than PDMS. This process can go on but all the processes after Fig. 2.5D share the same characteristics that the materials are soft (Ang et al., 2017) and the products made from the same pattern. For this reason, soft lithography is called.

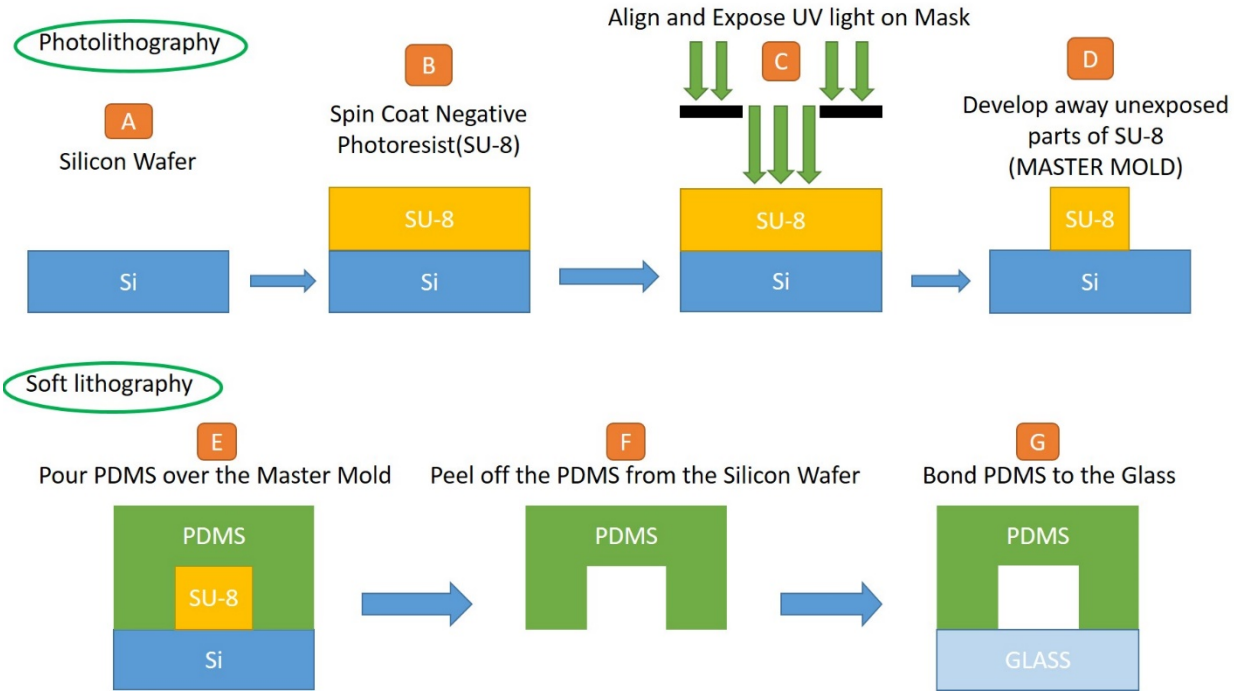

Figure 2.5 The procedure of Photolithography and soft lithography. (A)-(D) related to fabricating of the micro pattern structure using Photolithography. (E)-(G) would be related to soft lithography process which is using master mold and try to pattern the structure on a PDMS.

2.7 Conclusion

The above discussion can conclude that the proposed work, i.e., to develop a novel soft self-switch valve is original and some interesting contribution is expected to be made in the field of soft robots or soft machines in general (Sun, Yang, Zhang, & Zhang, 2011). This novel soft self-switch value extends the existing concept of switch valve.

Chapter 3 : Design of a Novel Soft Switch Valve

3.1 Introduction

This chapter presents design of a soft self-switch valve, which is in essence a fluid-deformation switch valve. This includes the requirement analysis, conceptual design and embodiment (including detail design) of the valve. It is noted that the outcome of conceptual design of a device is in fact design of the architecture of a device or the principle of a device (Adam et al., 2015).

3.2 Design requirement

To switch flow rate between fluid A and fluid B. Suppose flow A has rate RA and flow B has flow rate RB. The switch valve is required to fulfill: (1) RA (x% of a constant CA) and RB (y% of a constant CB), where x+y=100. When x=0 and y=100, no flow for A, but full flow for B, and vice versa.

The overall FR is decomposed into

- FR 1: to move the fluid A.
- FR 2: to move the fluid B.
- FR 3: to control the amount of A to B proportionally subject to OA+OB=100, where OA is the percentage of the opening of A and OB is the percentage of the opening of B).

FR 3 is further decomposed into

- FR 3.1: to connect the channel A and the channel B such that expansion of the channel A

leads to contraction of the channel B and vice versa.

- FR 3.2: to adjust the expansion and contraction of the two channels in a continuous manner (i.e., the channel does not completely close or open but follows the rule of OA+OB=100; see the previous discussion).

The constraint requirements (CRs) that identified for the new design is,

- CR1: The channels should be on micro scale.
- CR2: The membrane should be as flexible as possible in its lateral direction.

3.3 Conceptual or Concept Design

The design parameters (DP) of the device under design are determining by considering each function requirement along with each constraint requirement, and they are mentioned below.

- DP 1: A channel A with a membrane, in which the fluid A flows through from its inlet and to outlet and deforms the membrane in the channel A.
- DP 2: A channel B with a membrane, in which the fluid B flows through from its inlet and to outlet and deforms the membrane in the channel B.
- DP 3.1: A channel that connects the channel A and the channel B such that the deformation of the membrane in one channel affects, reversely, the deformation of the membrane in the other channel (i.e., if the channel A is closed, the channel B is open, and vice versa).

- DP 3.2: A third channel that connects the channel A and B, respectively, (see DP 3.1), in which a control fluid flows to maintain a pressure on the membrane of the two channels (A, B) so that the degree of the opening in the channels A and B can be controlled (i.e., they follow the rule of OA+OB=100, of which complete close and open are just a special case).

Figure 3.1 shows the structure of FR and DP. From Figure 3.1, one can get the following matrix (Suh, 1990; Fan et al., 2015), which shows that the design for FR 3 is a decoupled design and meets Axiom 1.

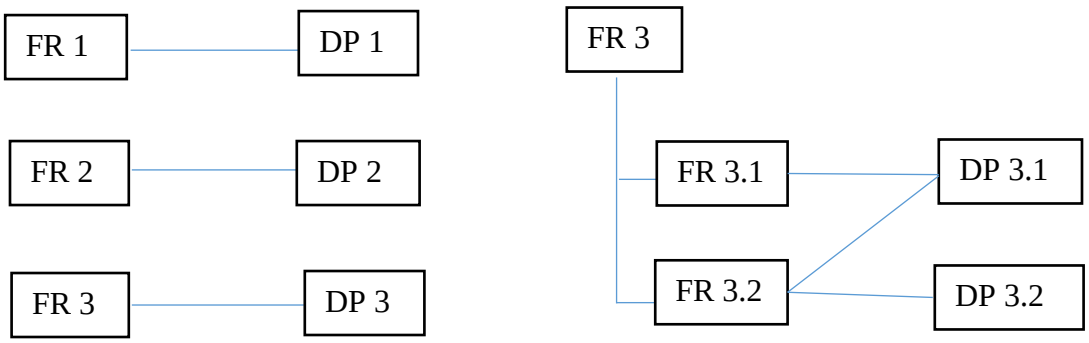

Figure 3.1 The relationship between the selected FRs and DPs.

$$\begin{bmatrix} FR1 \\ FR2 \\ FR3.1 \\ FR3.2 \end{bmatrix} = \begin{bmatrix} 1 & 0 & 0 & 0 \\ 0 & 1 & 0 & 0 \\ 0 & 0 & 1 & 0 \\ 0 & 0 & 1 & 1 \end{bmatrix} \times \begin{bmatrix} DP1 \\ DP2 \\ DP3.1 \\ DP3.2 \end{bmatrix} \quad (3.1)$$

From Equation (3.1), this design is a decoupled design, particularly with respect to the design for FR 3. Figure 3.2 integrates all the designs (DP1, DP2, DP3.1 and DP3.2). From Figure 3.2, there

are two fluids A and B, flowing in two channels, respectively, as well as the control fluid (i.e., the fluid C).

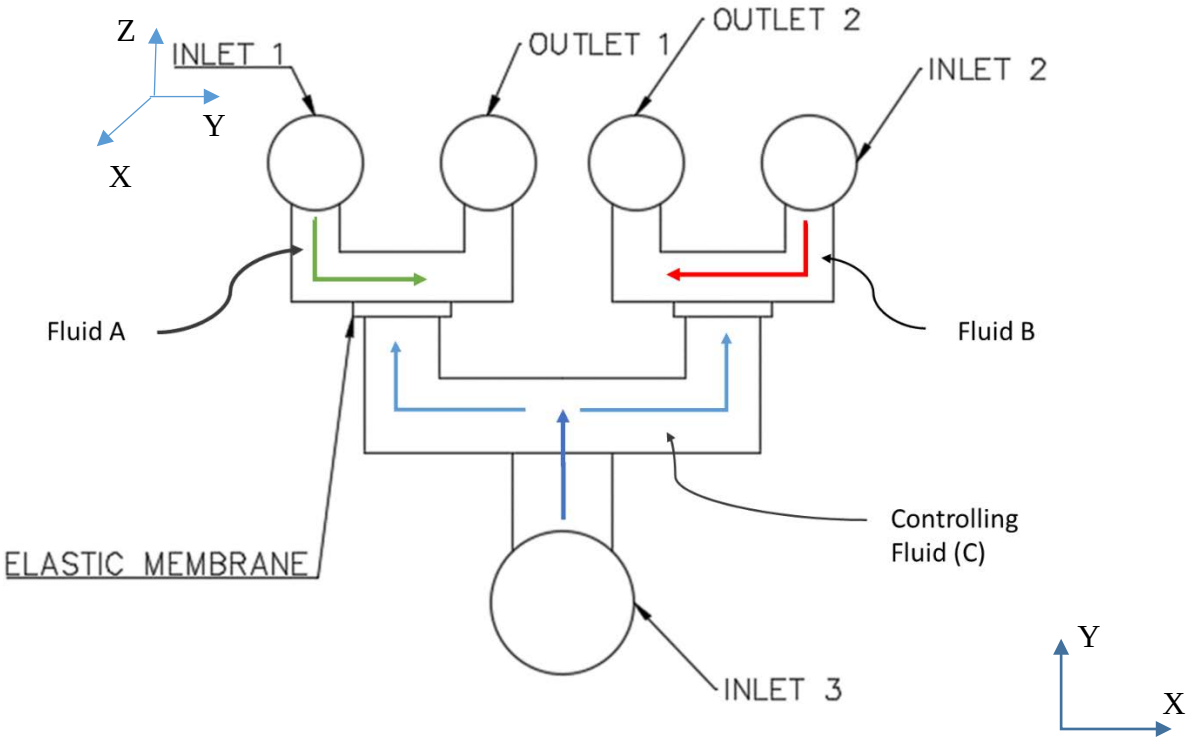

Figure 3.2. The integration of all the DPs. Z-direction is the gravity direction

The operation of the proposed device can be illustrated with the help of Figure 3.3. **Step 1**: pre-set the control fluid (C). **Step 2**: the fluid A flows into the channel A to deform the membrane in the channel A so as to open the channel A and the fluid A can flows through the channel and exits at its outlet, while at the same time, the membrane in the channel B deforms to close the channel B so that the fluid B is of no flow; this situation corresponds to State 1 in Figure 3.3**. Step 3**: the fluid B in the channel B builds up so as to increase the pressure in the fluid B, which subsequently deforms the membrane B to open the channel B, while at the same time, the membrane in the channel A deforms to close the channel A; this situation corresponds to State 2 in Figure 3.3.

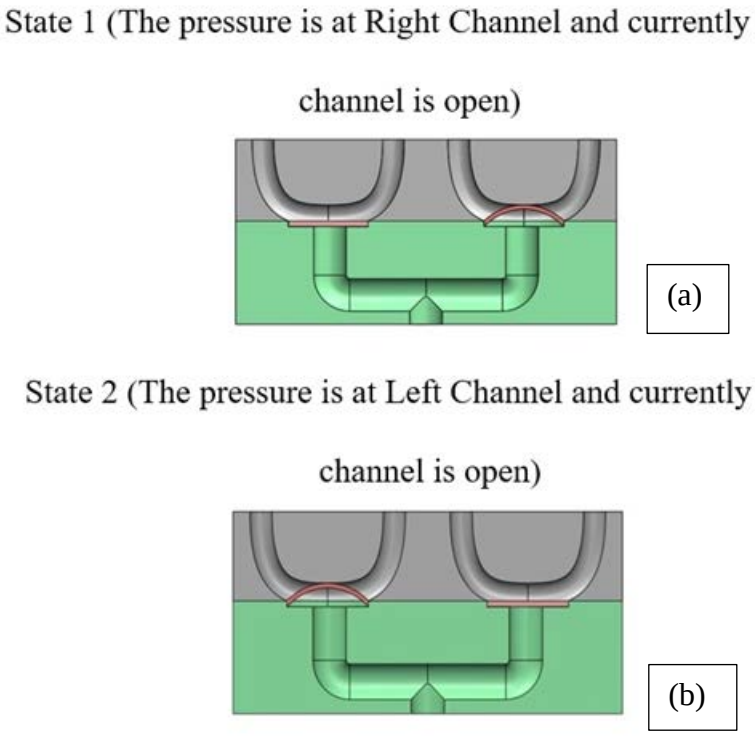

Figure 3.3 The function of the new Switch Valve. (a) In this condition, the pressure at the left channel is higher than the pressure at the right channel. Thus, the membrane in the left channel is pushed down while the membrane of the right channel is pushed up and closes the channel of the right channel. In this condition, only the fluid in the left channel can flow; (b) In this condition, however, the pressure of the fluid on the right channel is higher and this leads to the closing of the left channel and consequently the flowing of the left channel stops.

Remark 3.1: The proposed design is free of the challenge of the alignment of three layers in the micron accuracy, as all the components are placed in one layer (horizontal layer, X-Y plane). The leakage problem can be alleviated by reducing the number of layers, which is another common problem with micro-fluidic systems (Chueh et al., 2007).

Remark 3.2: The proposed design also come with the additional function, that is, both channels open but follow the rule of OA+OB=100. This can be achieved by the control fluid (C), which is straightforward.

3.4 Embodiment Design and Detail design

Figure 3.4 shows a schematic of the embodiment design. There are three pieces of components, and they are: a controlling channel, two main channels along with a membrane in each channel. All these components are laid out in the X-Y plane, i.e., horizontally rather than vertically, to avoid the difficulty of alignment and bonding of the three layers (Fig. 1.2). The material for the main channels as well as for the controlling channel is Polydimethylsiloxane (**PDMS**), and the material for the membrane is also PDMS. The total thickness of the device is 100μm and dimension for the membrane is 50 μm width and 12500 μm in length, the dimensions of the main channels, which are in contact with membrane, are: 300μm width and 12500 μm length. The overall size of the device is 74850 μm in width and 38919.02 μm in length. The exact structure and dimension of all the components can be found in Appendix A.

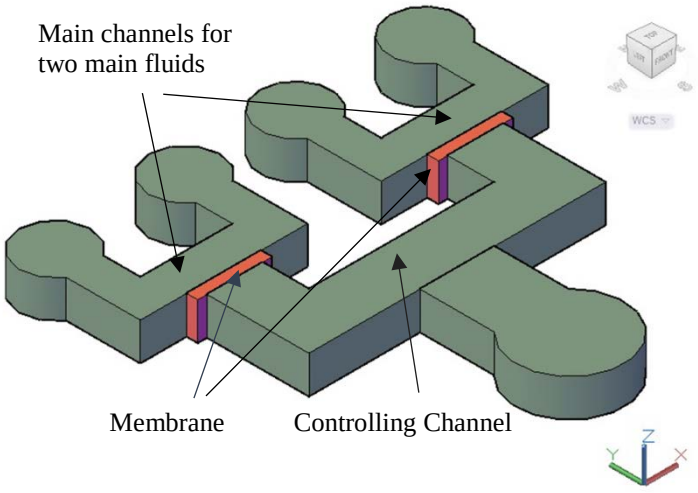

Figure 3.4 Embodiment design of the device

3.5 Conclusion

This chapter presents the design process along with the resulting design of a new soft self-switch valve or switch valve with embedded instructions. The new switch valve extends the traditional switching (i.e., 0-1 switching or open-close switch) to the switching that follows the rule of OA+OB=100, where OA is the opening of the channel A and OB is the opening of the channel B). Indeed, the nature of such a device is an integrated fluid and deformable channel system. The design content covers both the device design (i.e., deformation distribution design) and fluid design (i.e., the number of fluids, flow paths, pressures, flow rates, temperatures, and properties). It can be concluded from the discussion in this chapter that the proposed device is feasible to achieve the extended switching function.

Chapter 4 : **Modeling and Simulation**

4.1 Introduction

To gain confidence on whether the designed device works, simulation of the behavior along with performance of the device was conducted before fabricating the device. This chapter presents the modeling of the device. The theory of multi-physics device modeling was taken to develop the dynamic model of the device, including the fluid that flows on the device. The software COMSOL v.5.3a was used to implement the model and simulate the device. Due to the scope of this work, the modeling and simulation was restricted to examine the deformation of the membrane with different thicknesses and with different flow velocities of the fluid that flows over the membrane as well as channel. Section 4.2 presents the schematic model of the system to be simulated. Section 4.3 will overview the governing equation for the problem. Section 4.4 presents the model development in COMSOL environment. Section 4.5 presents the result of the simulation along with discussions. Finally, there is a conclusion in Section 4.6.

4.2 The Schematic Model of the Target System for Simulation

Due to the symmetric geometry, the simulation is performed on part of the device. Figure 4.1 shows the schematic model of the device for simulation along with its rationale. Figure 4.1a shows the original device, from which Figure 4.1b is derived because of the symmetric geometry of the device. In Figure 4.1b, Fluid 1 refers to the fluid in the controlling channel, and Fluid 2 refers to

the fluid in the upper left channel. Figure 4.1c is the final schematic model considered for simulation, where Fluid 1 and Fluid 2 are further merged into one fluid without loss of much accuracy because the two fluids are of the same type and their flows are both assumed as a laminar flow when they interact with the membrane.

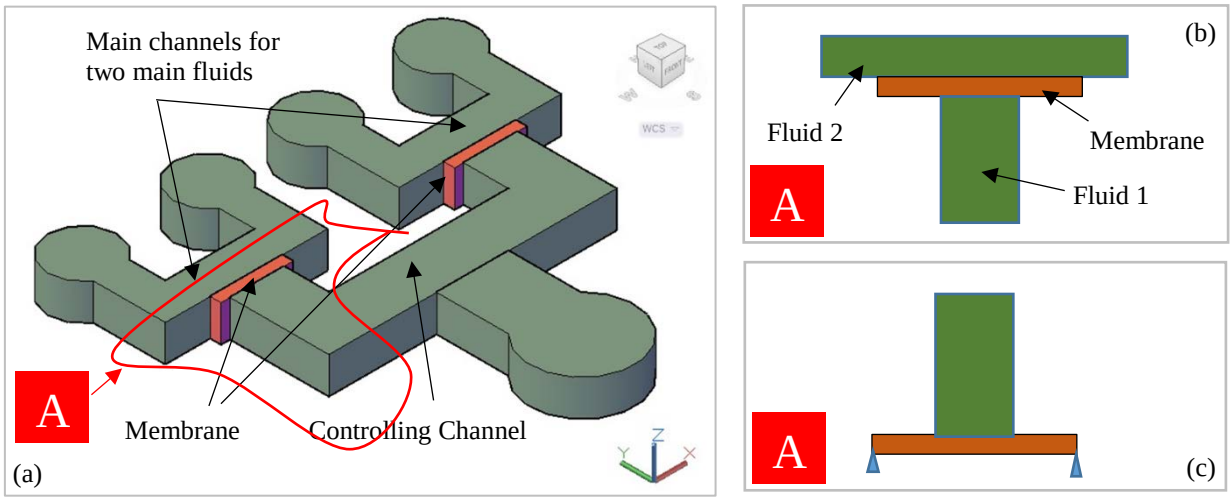

Figure 4.1 The Schematic Model of the Device: thickness: along Y-axis; width: along Z-axis, length: along X-axis.

4.3 Governing Equation

The system to be simulated is a fluid-solid system. The governing equation for such a system is presented in the following. First, PDMS is considered as a hyper-elastic material like rubber and its governing equation is given as follows (Yu & Zhao, 2009):

$$\rho\frac{\partial^2 \mathbf{u_{solid}}}{\partial t^2} = \nabla\cdot(F\,S)^T + Fv, \quad F = I + \nabla \mathbf{u_{solid}} \tag{4.1}$$

$$S = S_{ext} + \frac{\partial W_s}{\partial \epsilon}, \quad \sigma = J^{-1}FSF^T, \quad J = \det(F) \tag{4.2}$$

$$\epsilon = \frac{1}{2}\left(F^TF - I\right) \tag{4.3}$$

$$W_s = C_{10}(\bar{I}_1 - 3) + C_{01}(\bar{I}_2 - 3) + \frac{1}{2}\kappa(J_{el} - 1)^2 \tag{4.4}$$

where S is the second Piola-Kirchhoff stress tensor, and V is the volume, W is the strain energy density function, F is the force applied to the material, ε is the strain ratio, and C is the material constant. In this simulation, the value of C_{10} and C_{01} were taken as 0.07 MPa and 0.008 MPa, respectively, according to (Yu & Zhao, 2009).

Second, the fluid was considered incompressible, and the fluid flow was assumed to be a laminar flow. The governing equation is expressed by ("COMSOL Report," n.d.)

$$\rho\frac{\partial \mathbf{u_{fluid}}}{\partial t} + \rho(\mathbf{u_{fluid}} \cdot \nabla)\mathbf{u_{fluid}} = \nabla \cdot \left[-p\mathbf{I} + \mu\left(\nabla \mathbf{u_{fluid}} + (\nabla \mathbf{u_{fluid}})^T\right)\right] + \mathbf{F} \tag{4.5}$$

where p is the pressure of the fluid, u is the fluid velocity, ρ is the density of the fluid, and μ is the fluid dynamic viscosity. Also, due to the fact that the fluid was incompressible, we have:

$$\rho\nabla \cdot (\mathbf{u_{fluid}}) = 0 \tag{4.6}$$

Finally, in the fluid-solid interaction, the solid can be expressed by ("COMSOL Report," n.d.)

$$\sigma_{fluid} = -p_{fluid}\mathbf{I} + \mu\left(\nabla \mathbf{u}_{fluid} + (\nabla \mathbf{u}_{fluid})^T\right) - \frac{2}{3}\mu(\nabla \cdot \mathbf{u}_{fluid})\mathbf{I} \tag{4.7}$$

where σ is the stress tensor.

4.4 Model Development with COMSOL

The finite element approach was employed to solve the above governing equation, specifically with the help of the software COMSOL. COMSOL is specialized in solving multi-physics problems. Building of a finite element model of COMSOL (or Model for short in later discussions)

has the following steps. Step 1: create the geometric model of a target system to be analyzed. Step 2: define the material property to the geometrical model. Step 3: define the boundary condition and input condition. Step 4: mesh the domain.

Step 1:

Two different geometrical domains need to be defined according to the schematic model (Figure 4.1c), namely the fluid domain and solid domain, and their definitions are shown in Figure 4.2. With this schematic model, the four different thickness of the membrane were examined, and they are: 05µm, 10µm, 50µm, and 100 µm along with different widths, and also four different flow velocities, namely 0.1m/s, 0.5m/s, 1m/s, 1.5m/s, were examined.

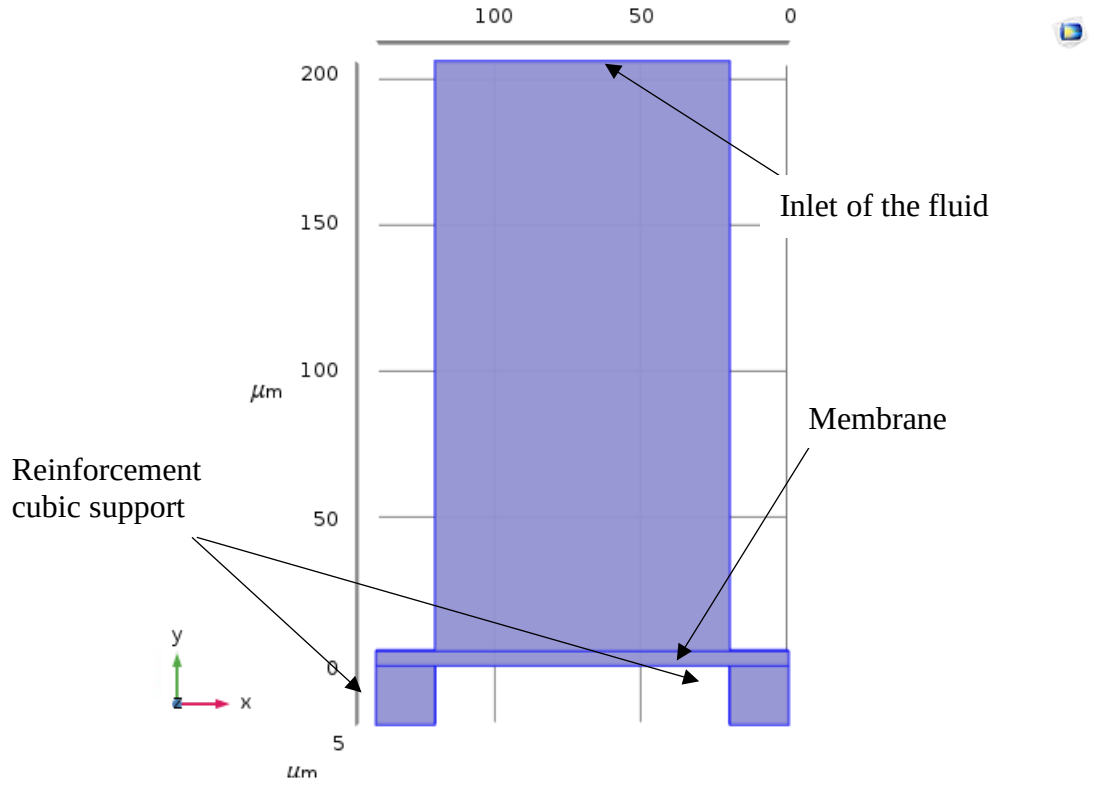

Figure 4.2 The Geometrical shape for the membrane that have been used. This is for the membrane's thickness of 05µm and the width of 10µm, length of 140µm with the velocity of 1.5m/s.

Thickness: along Y-axis; width: along Z-axis, length: along X-axis in reference to Figure 4.1. The fluid geometry is set to 200µm therefore the incompressible fluid can put enough amount of pressure on top of the membrane that can push the membrane further down. The fluid geometry amount can be increased as well but because it makes the rending and data analyzations hard and more time consuming in this study it is set to this amount.

Step 2:

The material for the two reinforcement cubic objects (in Figure 4.2) is PMMA. The reason of having this reinforcement here is that these two cubic objects can hold the membrane. The material for the membrane is PDMS. The type of fluid is water.

Step 3:

The fluid is assumed to be a laminar flow and incompressible. The geometry of the solid was considered unchanged. The inlet velocity of the fluid was specified to be four different velocities which were 0.1m/s, 0.5m/s, 1m/s, 1.5m/s to examine how the velocity may affect the deflection of the membrane.

Step 4:

The mesh was generated using the tool available in the software called “Fine”, and the result is shown in Figure 4.3. Further, the dynamic behaviors (fluid flow, stress in the membrane and deflection of the membrane) were examined via simulation, which was specified in the software by “Time-Dependent Fluid” and “Stress” and “deformation” of the membrane, respectively.

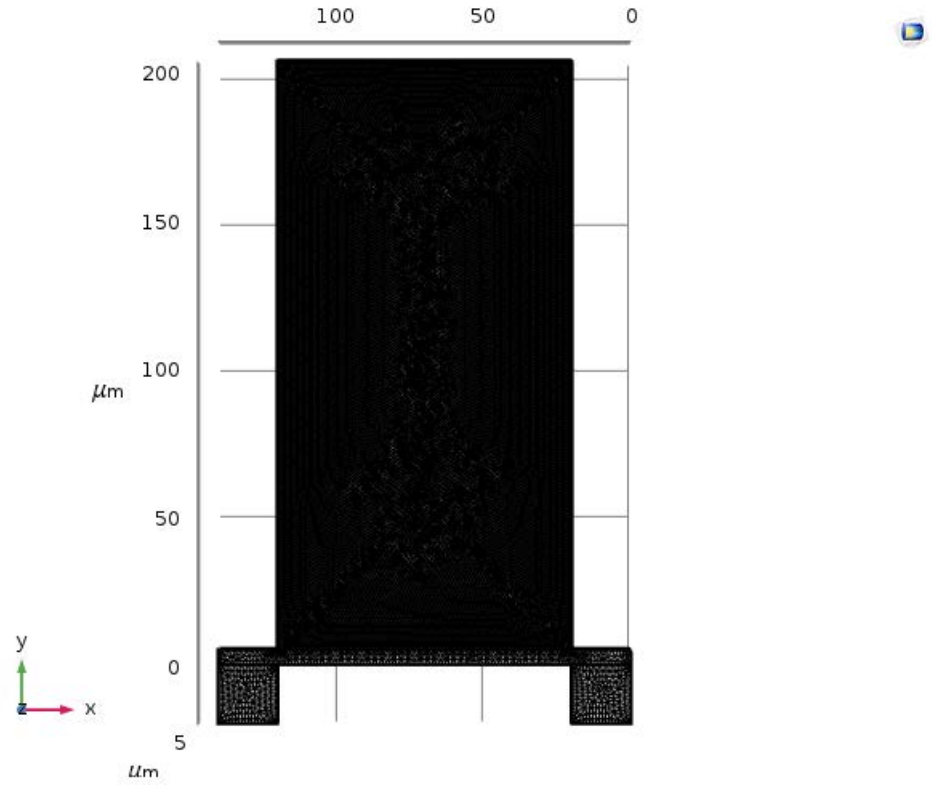

Figure 4.3 Meshing of the simulated device. This is for the membrane's thickness of 05µm and the width of 10µm, length of 140µm with the velocity of 1.5m/s. Thickness: along Y-axis; width: along Z-axis, length: along X-axis in reference to Figure 4.1.

4.5 Results and Discussion

First, the verification of the simulation model was carried out by comparing the simulation result with the measured result from a real system which will be discussed later in Chapter 5 and Chapter 6. Due to the restriction of the manufacturing resources to this study, only the membrane with the thickness of 50 microns can be made. Figure 4.4 shows both the simulation result and experimental result for the membrane with the thickness of 50 microns. Unfortunately, the plot cannot differentiate small deflections. Table 4.1 is provided, which shows both the simulation result and

experimental result. The RMSE between the simulation and experimental results is 4.07 µm, and this accuracy is acceptable and suggests that the simulation is valid and reliable. In Table 4.1, it shows that the trends of the simulation and experiment with the increase of the flow velocity are similar, which gives some confidence on the validity of the simulation. The microscope with the pixel link software(µscope) has been calibrated using Multifunction target calibrator (Model DA030) and the calibration result was 5.9 µm using the standard gauge. It is further noted that the instrument uncertainty is very high in the experiment, which is about 6.09 µm with the instrument and calibration (Appendix C). The error between the simulation result and experimental result is covered by the systematic and random uncertainty, which gives further confidence on the validity of the simulation. In the subsequent discussion, the simulation is used to prove the concept of this thesis.

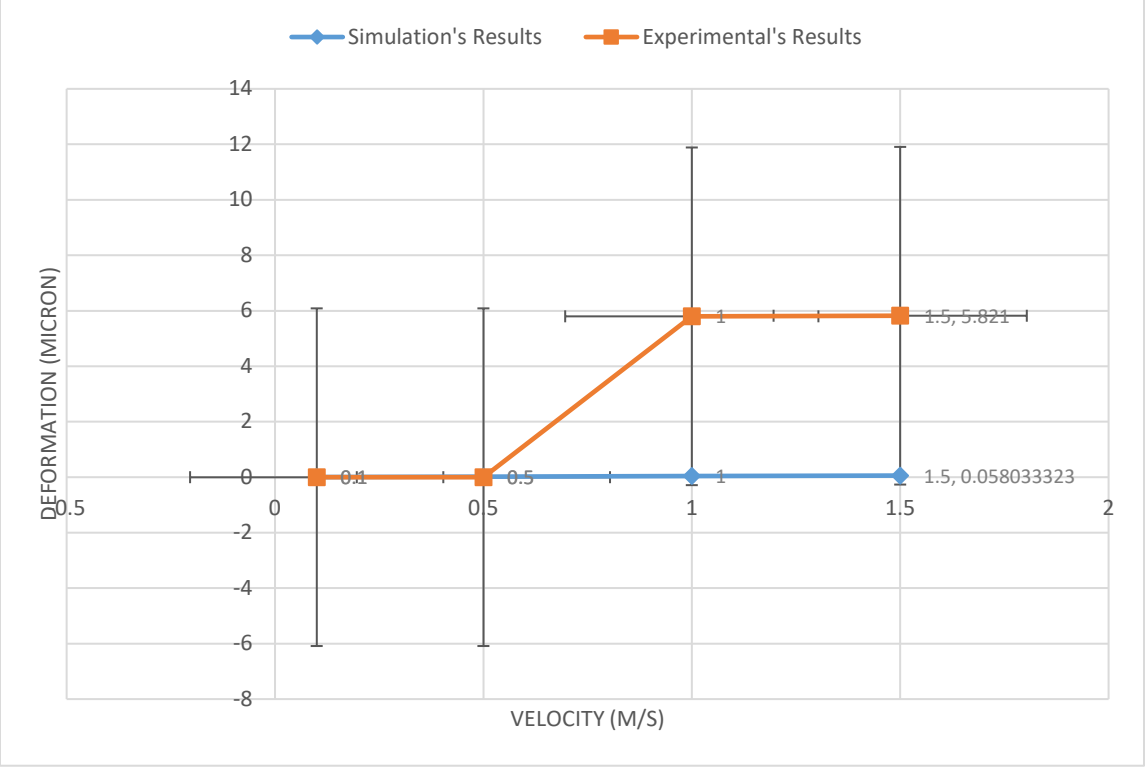

Figure 4.4 Comparison of the simulation and experimental results of the vertical deformation of PDMS membrane with its thickness of 50 µm versus different velocities.

Table 4.1 The amount of deformation between Simulation and Experimental results for the membrane with the thickness of 50µm, the length of 140µm, and the height of 25µm.

Velocity (m/s)	Simulation's Results (µm)	Experiential's Results (µm)
0.1	0.004	0
0.5	0.019	0
1	0.037	5.2
1.5	0.058	5.82

Figure 4.5 shows the result of the deflection of the membrane with the thickness of 05 µm, width of 10µm, and length of 140 µm, and flow velocity of 1.5 m/s. The maximum deflection is 14.299µm. Note that the channel size (along the Y-axis with respect to Figure 4.1) is about 13 µm, so the deflection is sufficient to close the channel to perform the switching function.

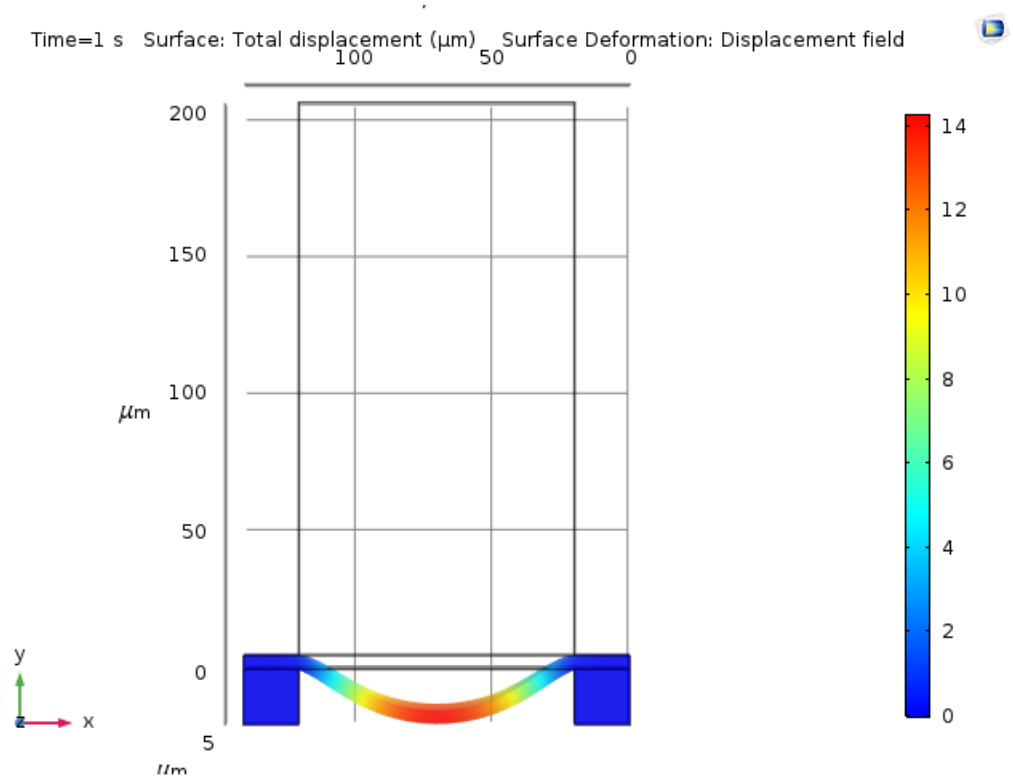

Figure 4.5 Deflection of the membrane with the membrane's thickness of 05 µm, width of 10 µm, length of 140µm, and the velocity of 1.5 m/s. In this figure the Y axis is the thickness, Z axis is the width, and the X axis is the length of the device in reference to Figure 4.1. All the dimensions in the figure are in microns (µm).

Fig. 4.6 shows the deflections of the membrane with the thickness of 05 µm, the width of 10 µm, and the length of 140 µm versus different flow velocities. The channel size (along the Y-axis) is 13 µm. Specifically, Figure 4.6A shows that with the velocity of 0.1 m/s, the channel is closed by 18 percent, 57 percent with the flow velocity of 0.5 m/s (B), and 86 percent the flow velocity of 1 m/s (C), and finally, the channel is completely closed with the flow velocity of 1.5m/s (D). Fig. 4.7 – Fig. 4.10 show the deflection of the membrane with the thickness of 5, 10, 50, 100 µm versus different widths and different velocities. All the results show a consistent behaviour of the membrane, which gives some assurance of the reliability of the simulation system with COMSOL.

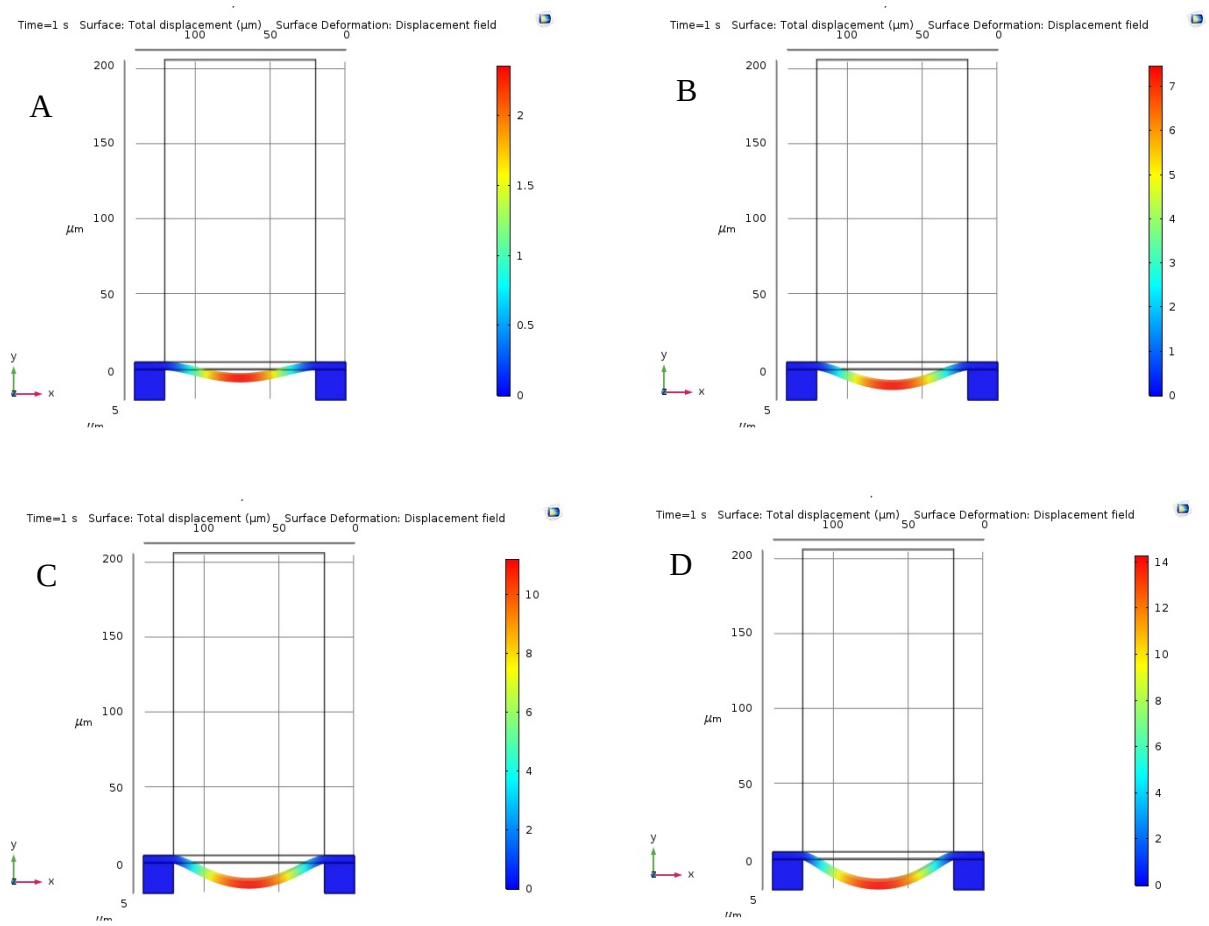

Figure 4.6 Deflection of the membrane with its thickness of 05 µm, width of 10 µm, length of 140µm, and the four different velocities. A) deflection of the membrane (2.36 µm) with the velocity of 0.1 m/s; B) deflection of the membrane (7.48 µm) with the velocity of 0.5 m/s; C) deflection of the membrane (11.22 µm) with the velocity of 1m/s; D) deflection of the membrane (14.30 µm) with the velocity of 1.5m/s; the Y axis is the thickness, Z axis is the with, and the X axis is the length of the device; all the dimensions are in microns (µm).

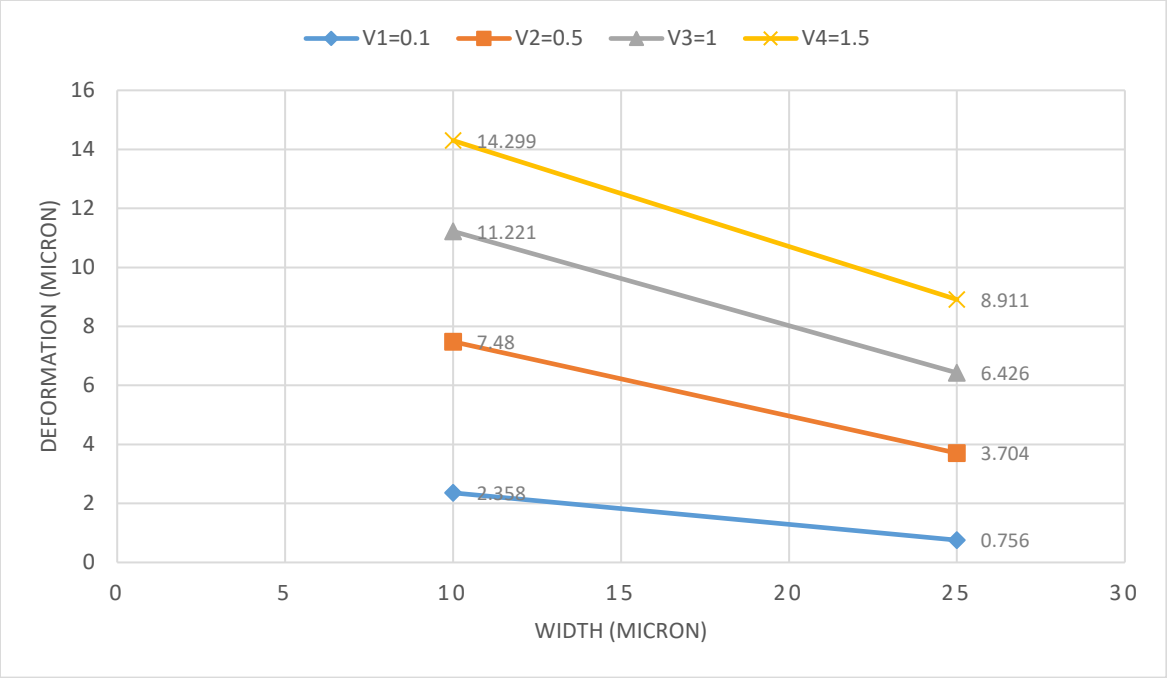

Figure 4.7 Vertical deformation of the PDMS membrane with its thickness of 05 µm and different widths and different velocities.

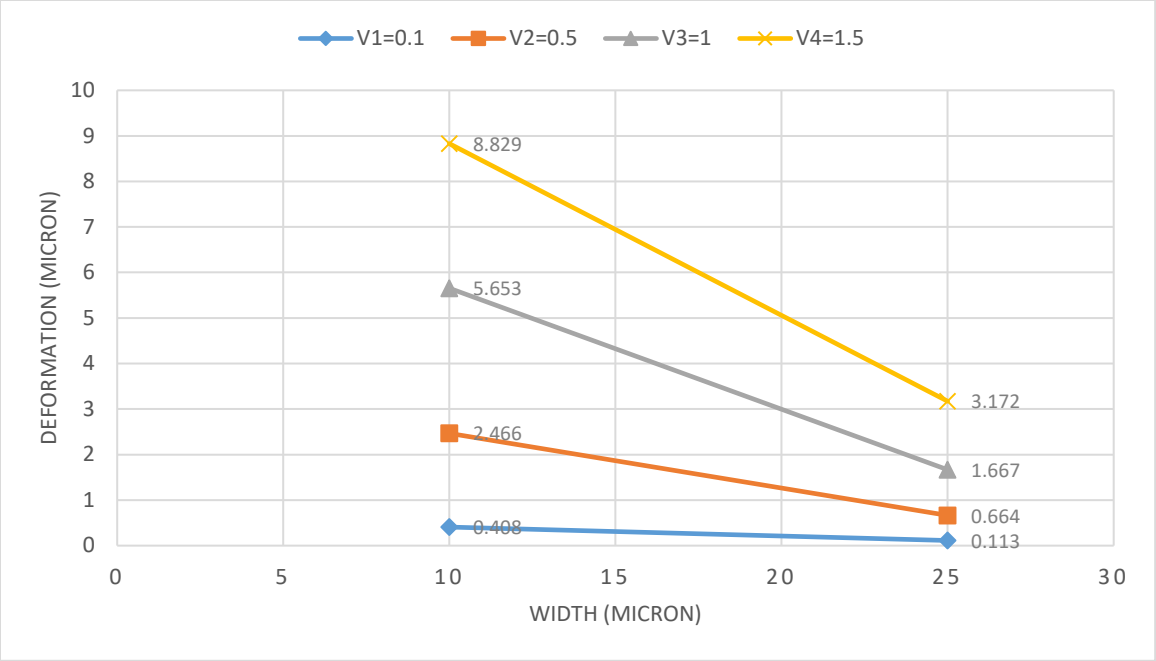

Figure 4.8 Vertical deformation of the PDMS membrane with its thickness of 10 µm different widths and different velocities.

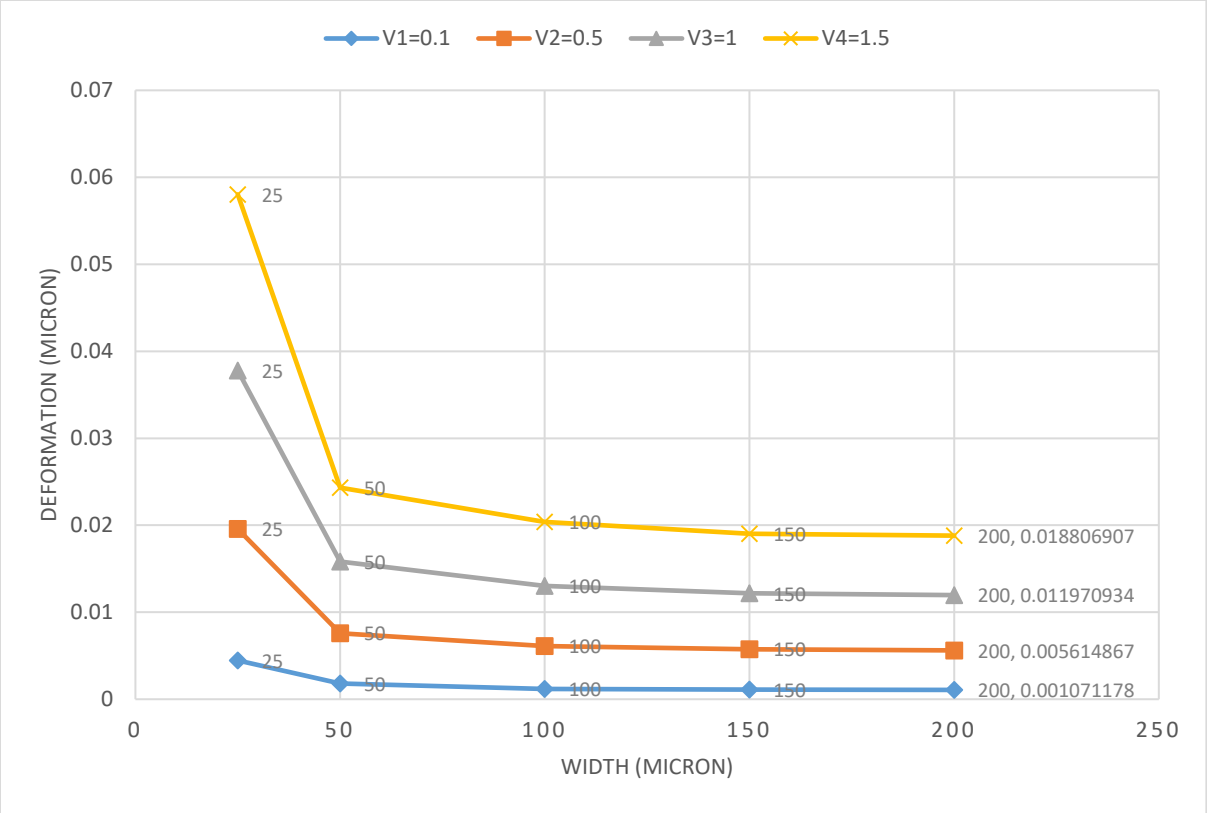

Figure 4.9 Vertical deformation of the PDMS membrane with its thickness of 50 µm and with different widths, and different velocities.

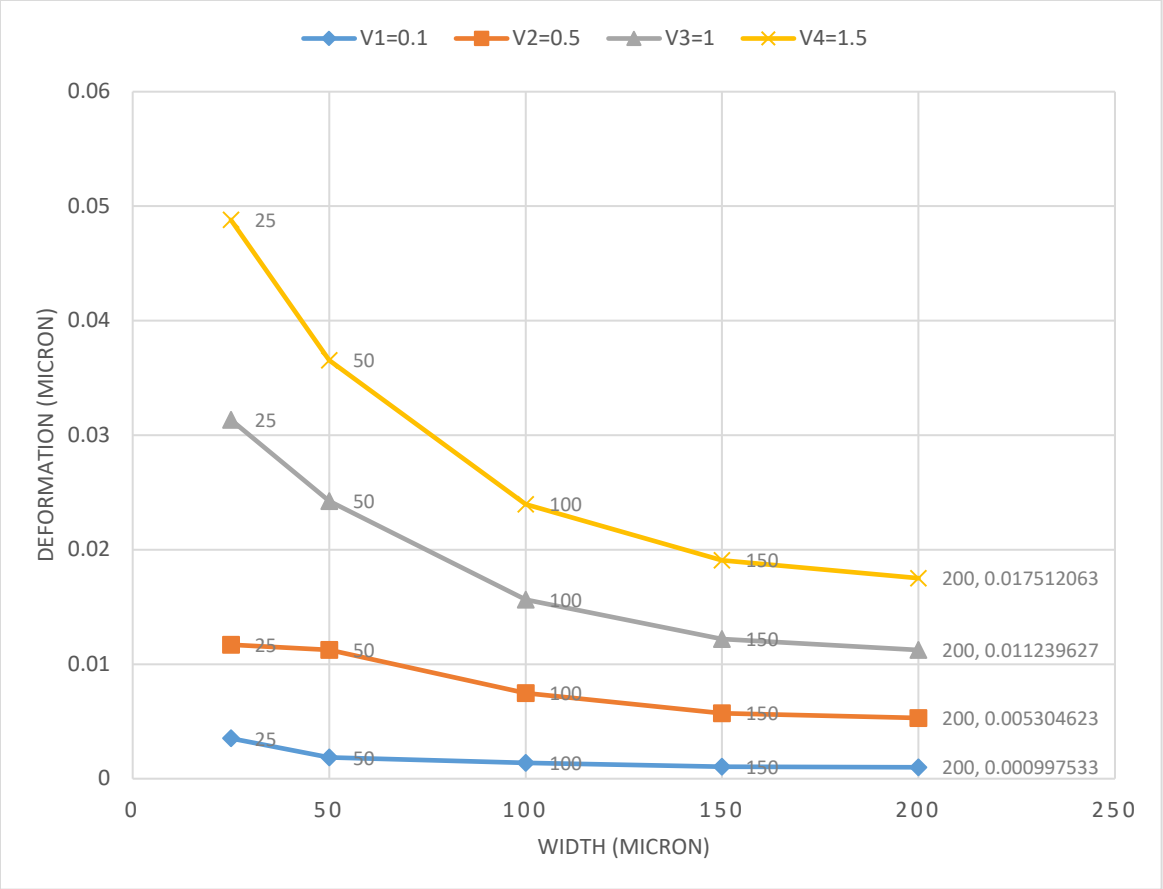

Figure 4.10 Vertical deformation of the PDMS membrane with its thickness of 100 µm, different widths, and different velocities.

4.6 Conclusion

In this chapter, the simulation of the fluid and PDMS membrane was described. From the simulation, it can be concluded that the membrane can have enough deflection to completely close the micro-channel. The simulation model was validated by a preliminary experiment which will be described in Chapter 5, as the deflection of the membrane changes with the velocity of the fluid over the membrane; specifically, an increase of the velocity of the fluid will cause an increase of the deflection of the membrane. Another evidence that the simulation model is valid is that the

deflection of the membrane is sensitive to the thickness of the membrane; specifically, if the thickness of the membrane decreases, the deflection of the membrane increases.

Chapter 5 : Fabrication and Assembly

5.1 Introduction

In this chapter, the fabrication and assembly of a prototype of the device described in Chapter 3 (especially Figure 3.4) are presented. It is noted that the prototype is not the whole device but part of it, as described in Figure 4.1b (Chapter 4). The fabrication and assembly were made at the Canadian Light Source (CLS) facility located in the Saskatoon, SK. Section 5.2 presents the fabrication and Section 5.3 presents the assembly. There is a conclusion in Section 5.4.

5.2 Fabrication

The fabrication process followed Figure 2.5. There are several steps to complete the fabrication.

Step 1: to make the photomask.

The photomask was built by a laser machine ("Heidelberg Instruments DWL 66+," n.d.) (Fig. 5.1A), because this machine is quite accurate according to the ("Heidelberg Instruments DWL 66+," n.d.), the resolution and the accuracy of this machine is as high as 0.3μm which satisfies the need of this study. The result of the photomask is shown in Fig. 5.1B.

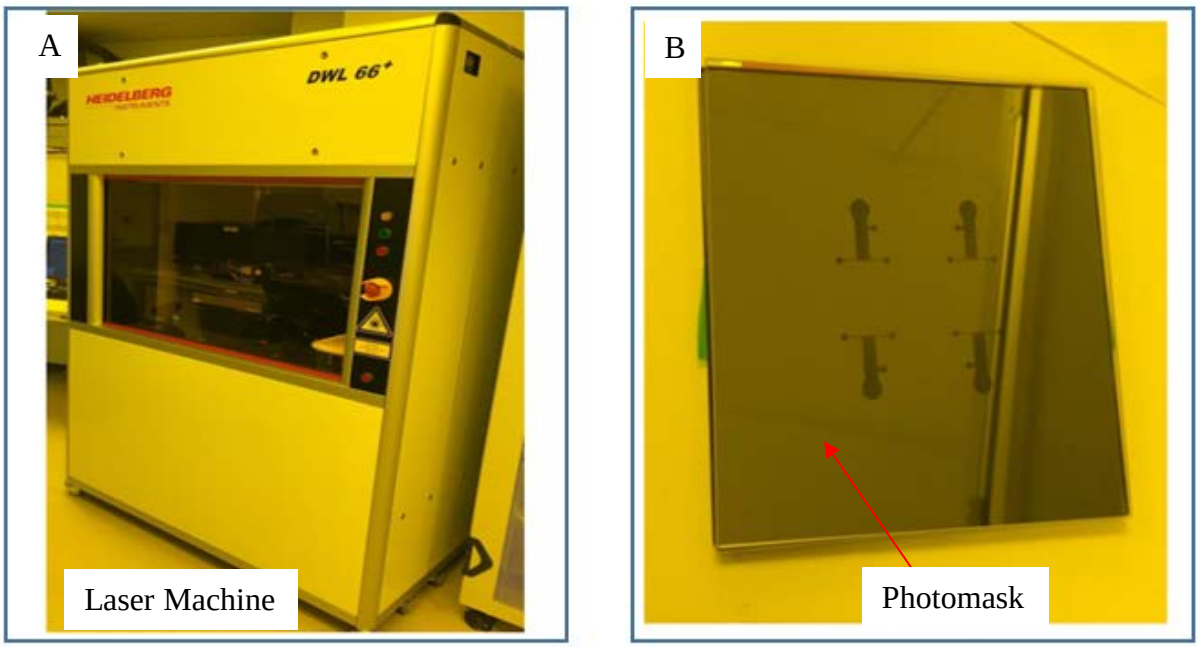

Figure 5.1 The Laser Machine and the photomask. A. The laser Machine that have been used for making the photomask. B. The photomask which have been created with the laser machine.

Step 2: Coat the negative photo-resistance on silicon wafer.

In this study, the material called SUEX (Sheet, n.d.) was chosen because it is a dry resistant and that makes it much more uniform in terms of surface in comparison with SU-8 which ultimately leads to having a better and uniform channels and structures after UV exposure. A hot-roll lamination machine (Table Top Roll Laminator RSL-2702) was used. The upper temperature (167^{o}F) and lower temperature (176^{o}F) were chosen based on the experience. It should be noted that the SUEX sheet plate should be put in the middle of the silicon wafer and underneath of the hot roller. The temperature on the roller should be higher than the room temperature. It is also noted that the temperature of the wafer needs to be cooled down to the room temperature before proceeding to the next deposition. Figure 5.2 shows the outcome of this step.

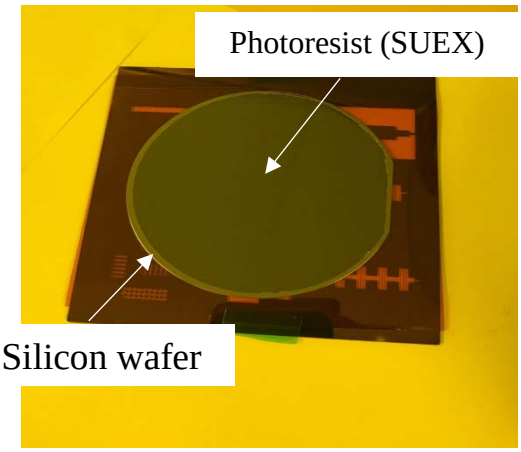

Figure 5.2 Silicon wafer that is coated with SUEX

Step 3: Exposure of the UV light on the photo-resistive material.

The silicon wafer with the SUEX coating along with the photomask was put inside the chamber of UV light exposure. The UV light machine was UV light source Series30, Atand. For the exposure, the dose was chosen to be 1320 mJ and it was exposed for 300 seconds at 4.4 mW. After that, the whole system was put for baking. The baking temperate was 85^{o}C, and the duration of baking was 1 hour, and finally it was cooled down to the room temperature (25^{o}C) for eight hours.

Step 4: Development.

Prepare for two baths: clean bath and dirty bath (Figure 5.3). Both were filled with the same development material. The UV exposed photo-resistive system was first put in the clean bath for 6 minutes and then in the dirty bath for 10 minutes. Finally, it was put in the Isopropyl alcohol (IPA) solution for 5 minutes, then 2 minutes in H_2O, then dry it completely. Figure 5.4 shows the result of the device fabricated at this point, which is also called master mold, corresponding to Figure 2.5D, for the follow-up soft lithography process.

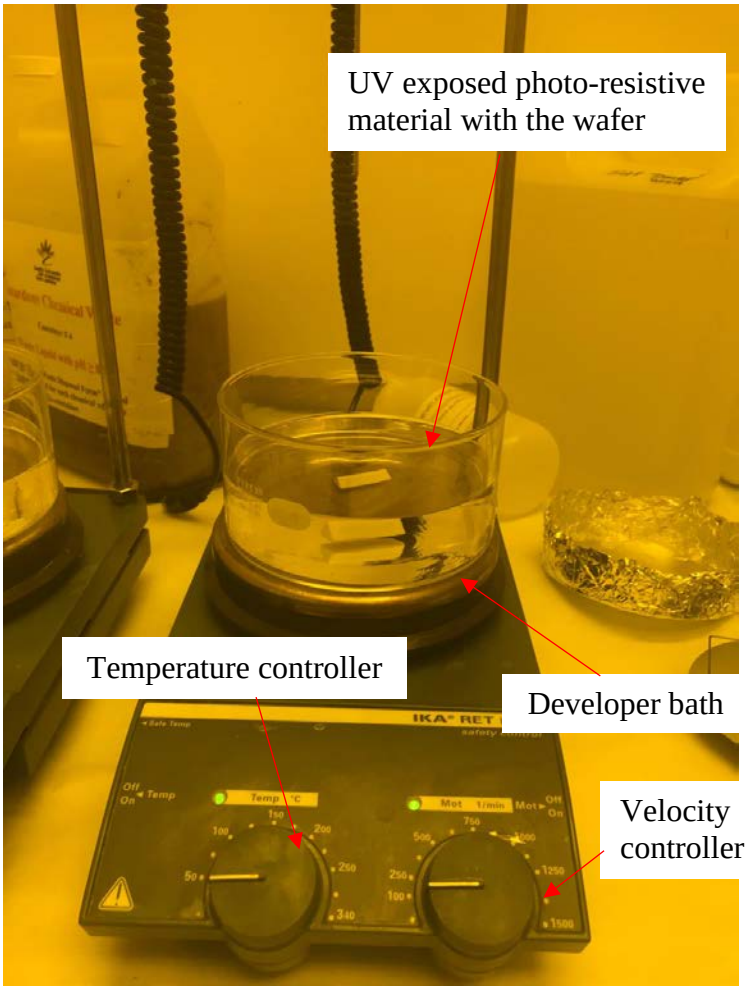

Figure 5.3 Developer's Bath for the development of the silicon wafer after the post-exposure bake.

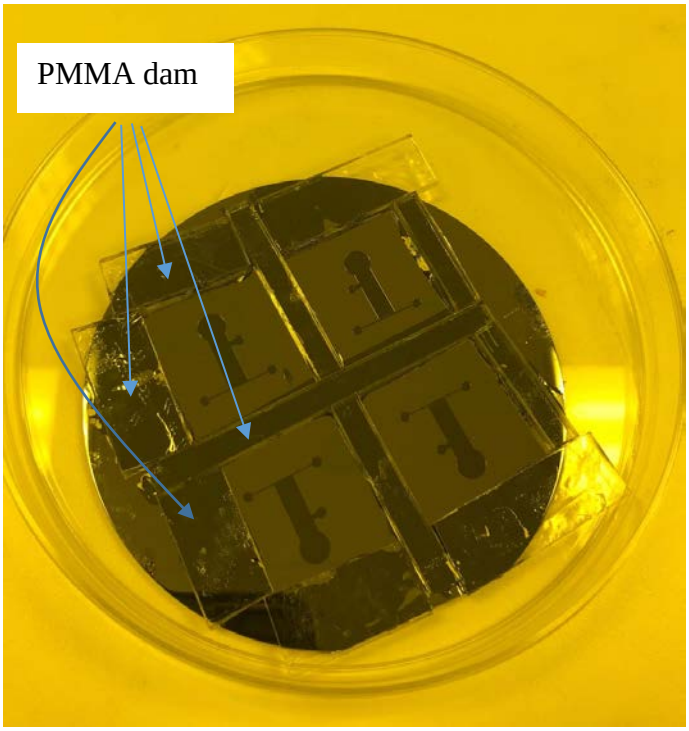

Figure 5.4 Master mold that has 4 pieces of the device which varies in terms of thickness of the membrane.

Step 5: Making the channel and membrane.

Began with the soft lithography process (Figure 2.5E). Step 5a: prepared PDMS melt. Specifically, mixed PDMS by the curing ratio of 1:10 completely (15 mL of the PDMS for four devices); put the mixed PDMS into a vacuum chamber to remove the air bubble. Step 5b: poured the PDMS on the silicon wafer and cured the poured PDMS with the silicon wafer at room temperature for 24 hours. Step 5c: peeled of the PDMS. Figure 5.5 shows a schematic diagram of the PDMS channel with membrane. Figure 5.6 shows the result of the PDMS channel and membrane.

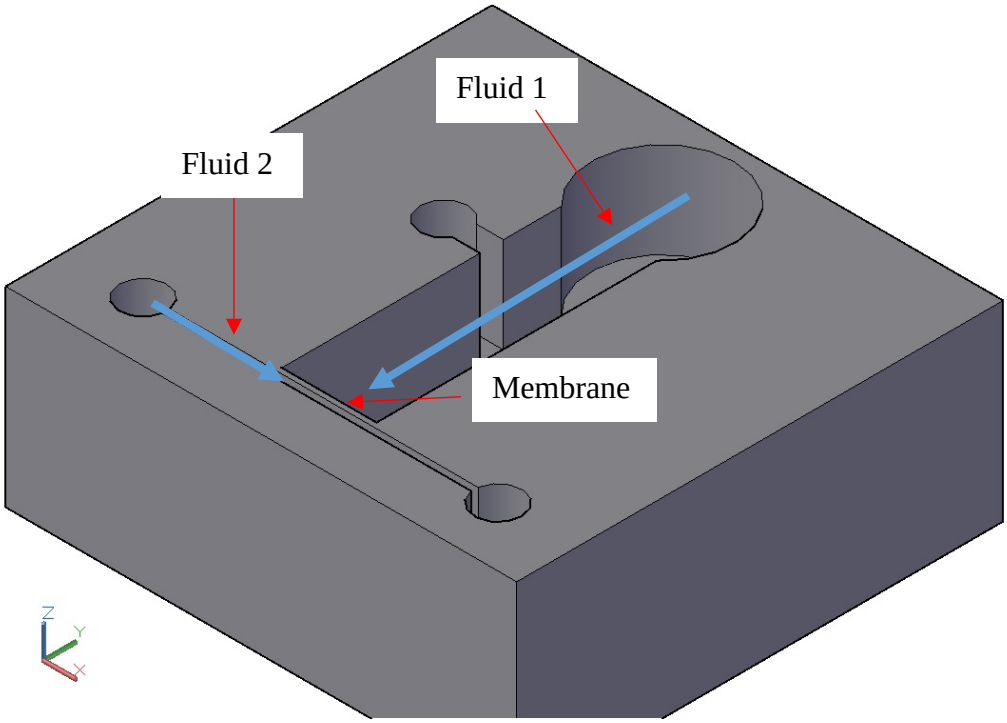

Figure 5.5 The schematic diagram of the device which has two channels and the membrane is the space between two channels the fluid goes on the top channels and put pressure on the membrane and try to push the membrane down.

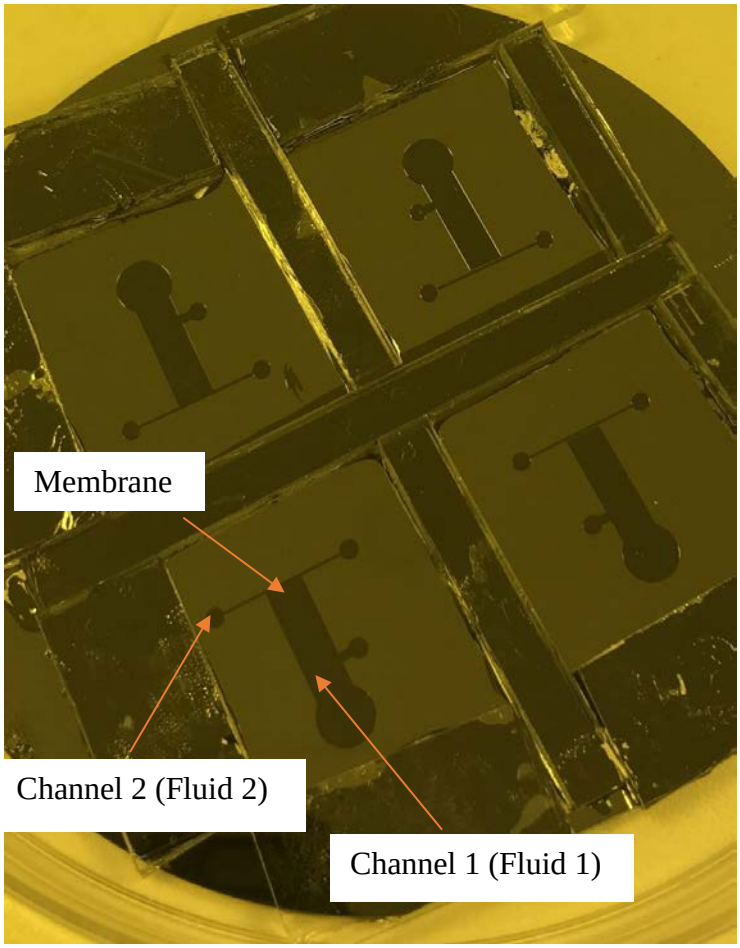

Figure 5.6 there are four different PDMS molds that has been getting from the silicon wafer and ready for the bonding to the glass.

5.3 Assembly

The PDMS channel needs to be covered, and this can be achieved by bonding it to a glass plate. The bonding was fulfilled with the oxygen plasma machine with the setting as 50 watts for 44 millitorrs of O_2 for 30 seconds (Fig. 5.7). After bonding, the whole device was put in the oven at

85ºC for 25 minutes. The bonding strength was tested by having a needle to move the PDMS to see if it may be peeled off otherwise, the bonding strength was considered enough. The needle was with the following specification: PrecisionGlide™ Needle 30G×1/2 (0.3mm×13mm). Figure 5.8 shows the result of the device after bonding. In Fig. 5.8, two of the PDMS samples can be observed, which is bonded to the glass.

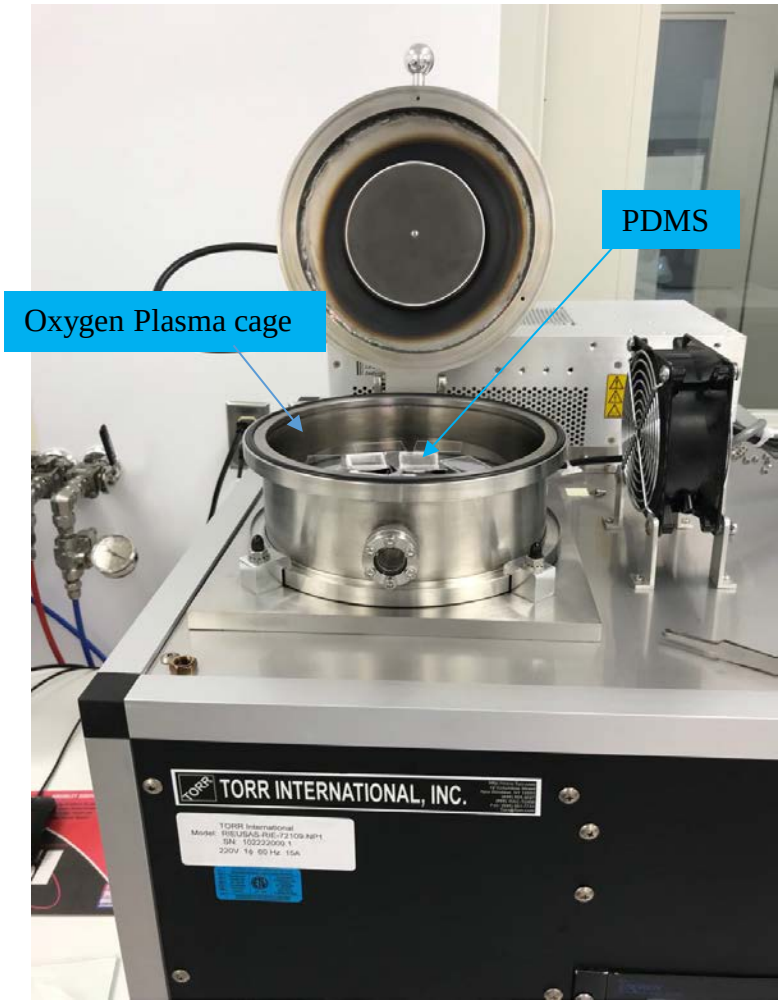

Figure 5.7 The oxygen plasma that has been used for bonding the PDMS to the glasses.

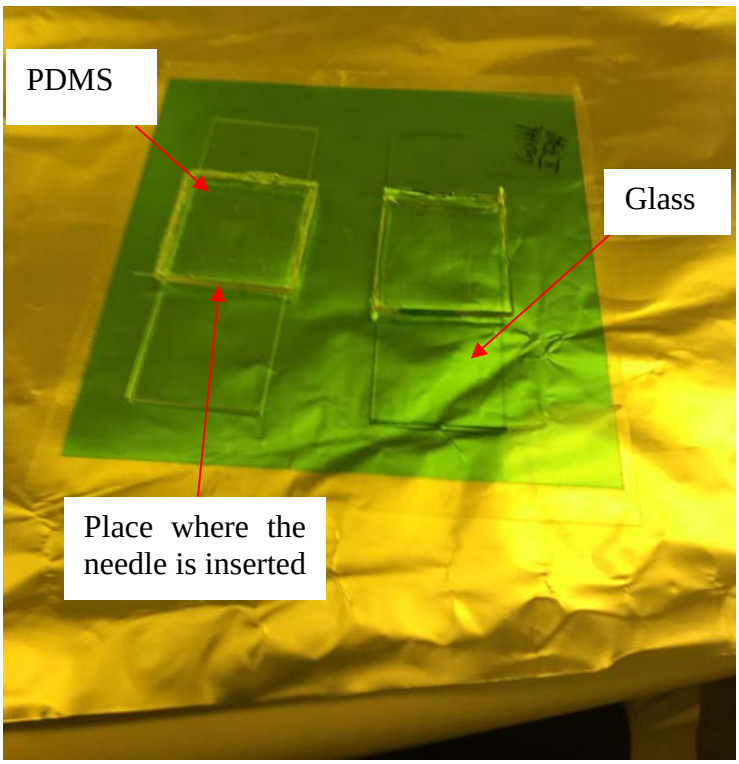

Figure 5.8 two of the PDMS membranes which have been bonded to the microscopic glasses.

5.4 Conclusion

This chapter presented a complete fabrication process based on photolithography and soft lithography. PDMS was used to build both channels and membrane, due to its cell compatibility. It can be concluded that the proposed design can be fabricated. The whole fabrication and assembly process is far simpler than the one presented in (Mosadegh et al., 2010). However, there are some limitations with the fabrication of the device. The first limitation is that the glass and the bottom of the channel stick partially, so the clearance for the fluid to flow becomes very difficult. The second limitation is that the thickness of the membrane is far from the required thickness, which is 05µm according to the simulation result (see Chapter 4).

Chapter 6 **: Experiment**

6.1 Introduction

In this chapter, the experiment is described. A preliminary observation found that deflection of the membrane was very small, because the fabrication was unable to make the membrane with the thickness of 5 μm (as discussed before in Chapter 5). The measurement was only performed on the membrane with the thickness of 50 μm. The deflection of this membrane is very small (see Table 4.1), which is certainly beyond the resolution of the measurement tool (~5.9 μm) (see Appendix C). Therefore, the measurement has a great uncertainty, and often only the trend of information was available. The quality of the channel was also poor, so the quantitative measurement of the flow velocity was not attempted. Section 6.2 describes the experimental set-up. Section 6.3 presents the experimental result with some discussions. Section 6.4 gives a conclusion. Appendix C describes the calibration of the measurement tool which is image-based.

6.2 Experiment Setup

The experimental set-up is as follows. A microscope or micro-lens (CAMKIX D0310-3LL-BLA) with at least 10X magnification was used to visualize the deflection of the membrane and flow of the fluid in the channel (see Figure 6.1a). The optimal focal distance from your viewing subject for this micro-lens is about 12mm. The fluid was coloured by food colour preparation (House Club brand). A syringe (Syringepk010) (Figure 6.1b) was used to pump the fluid into the channel. A

needle (BD PrecisionGlide™ Needle 30G×1/2 (0.3mm×13mm)) (Figure 6.1c) was used as a kind of valve on the syringe. The operation on the fluid was performed manually, because the channel was too small and coarse, preventing any meaningful use of the pump and valve.

The schematic diagram of the device in the experiment set-up was shown in Figure 6.2. In this figure, Fluid 1 was pumped into the main channel (also called Channel 1), and the flow of this fluid is expected to press the membrane to deflect so as to affect the flow of Fluid 2 which was in the side channel (also called Channel 2). It is noted that how the deflection of the membrane may affect Fluid 2 was not measured in this study because of two reasons. First, the deflection of the membrane is too small (due to the thickness of the membrane is too big, which is further because of the limitation of the fabrication facility available at CLS). Second, pumping Fluid 2 (as well as Fluid 1) was very difficult, observed in the experiment, due to sticking between the glass and the bottom of the channel and thereby very small clearance for the fluid to move.

Figure 6.1 Instruments used in the experiment. (a) micro-lens, (b) syringe, (c) needle.

The procedure of the experiment is as follows. The syringe was filled with the sufficient amount of colored water (1 mL in this experiment) based on the experience. The needle was attached to the syringe to squeeze the water out from the syringe into the main channel. In the meantime, the micro-lens was taken to observe the deflection the membrane.

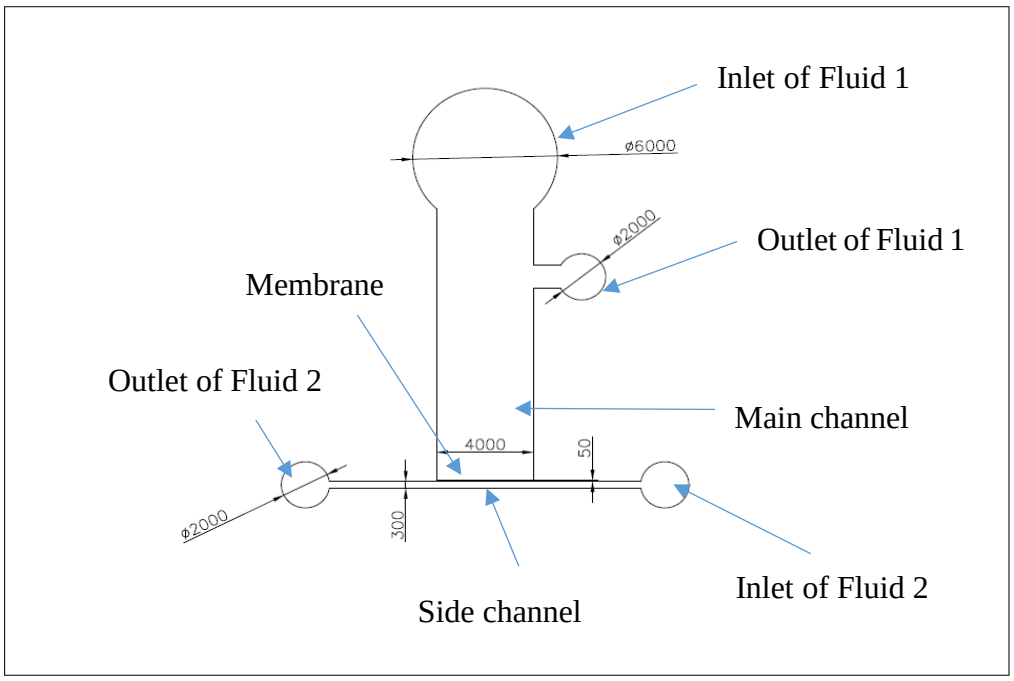

Figure 6.2 A sample of one of the membranes with the size of 50 µm in thickness of the membrane.

6.3 Results with Discussions

By inserting the needle into the syringe and inserting the deionized water inside the channel, deflection of the membrane can be observed. The injection of the colored water onto the main channel of the membrane can be seen in Figure 6.3. After injecting the colored water into the main channel by using the syringe, the deflection of the membrane was observed, which was about 0 µm at the initial spot and little by little it increased to 5.82 µm with the increase of the pressure; see Figure 6.4E and Figure 6.4F. It is noted that the pressure increase was sensed empirically by squeeze more water into the main channel. By the way, the results here were also documented early in Table 4.1.

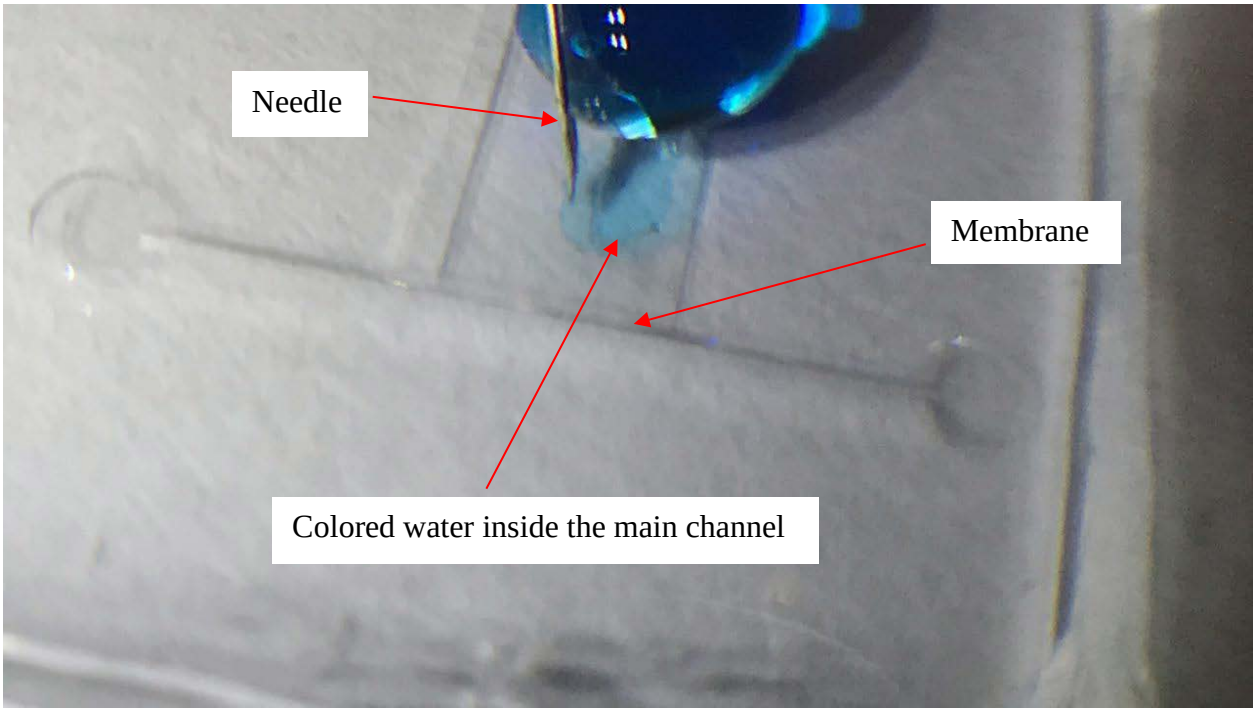

Figure 6.3 injection of the colored water into the main channel by using the needle.

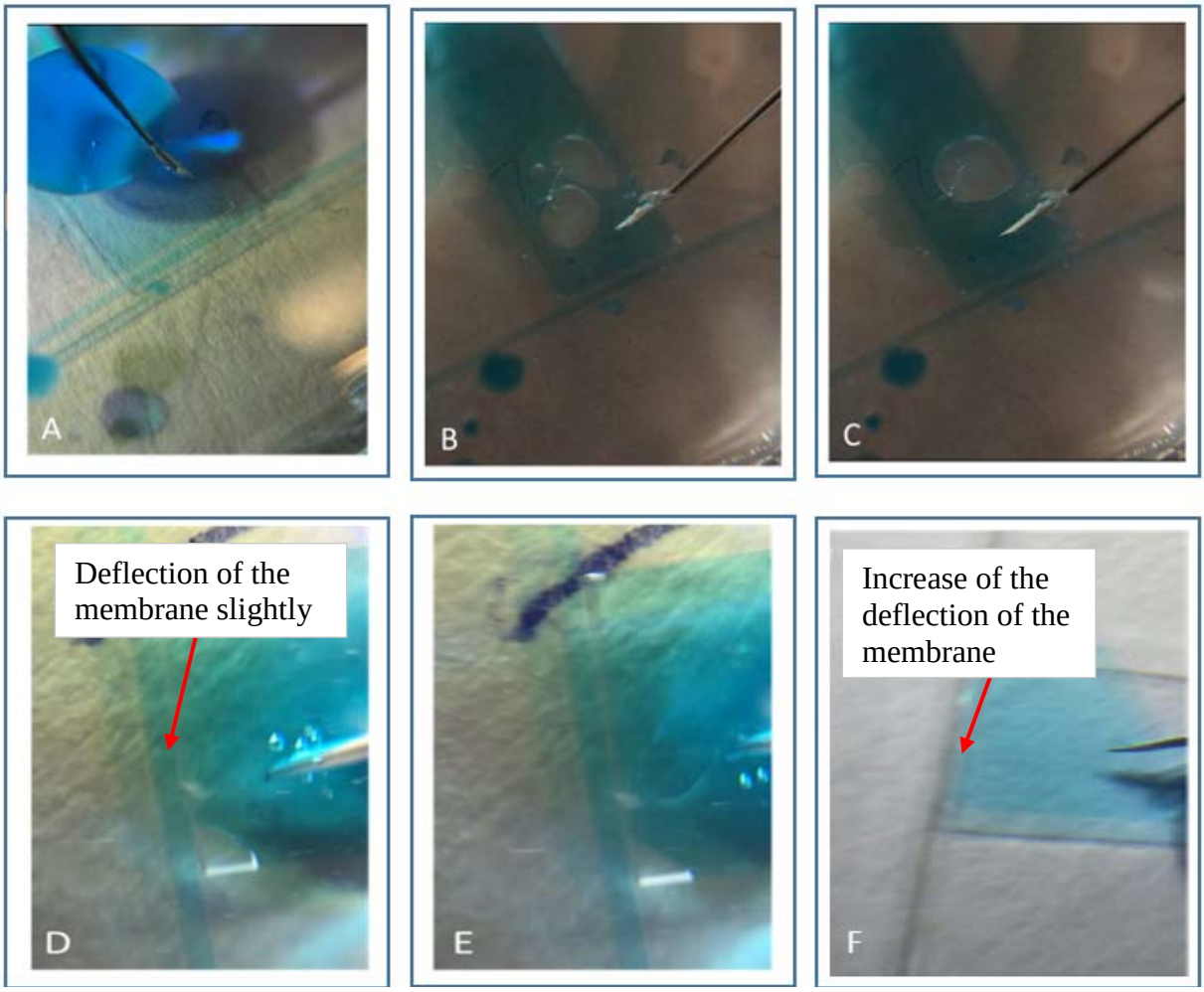

Figure 6.4 The examination of using a 30G needle and colored fluid. In the pictures above by injection of the fluid inside the main channel, small deformation of the membrane can be observed. From the A-F, the small deformation of the membrane can be seen. (A) the colored water is injected and all of the top and the bottom channels of the membrane are filled with the colored water. (B, C) with the help of the needles all of the areas which has small air inside will be taken away and filled with water instead. (D) a pressure is increased with the help of the needle and by inserting more colored water. Therefore, small amount of movement is observed where a membrane touches the other channel. (E, F) The movement continues as the pressure was increased by the needles.

6.4 Conclusion

In this chapter, the experiment was presented. Given the limitation of the measurement tool as well as the limitation of the fabrication (see Chapter 5, especially Section 5.4), the experiment had to be restricted to observing whether there was a deflection of the membrane and whether the deflection increases with the increase of the pressure of the fluid in the main channel. The deflection of the membrane was observed, and it was also obverted that the deflection of the membrane increased with the increase of the pressure of the fluid in the channel. However, a care must be taken that all the measurements in the experiment are qualitative. The quantitative information is only directive to the trend of information; yet it proves the concept of design and gives assurance of the reliability of the simulation as described early in Chapter 4.

Chapter 7: Conclusion and Recommendation

7.1 Overview and conclusion

The so-called integrated microfluidic circuit (**IMC**) is a relatively new field, which is an inter-discipline of deformation or solid mechanics and fluid mechanics. In the IMC, the deformation of the channel network and the flow of the fluid are coupled into a circuit to perform logics functions. The generic feature of such a system is integration of the deformation of the infrastructure and the flow of the fluid in the infrastructure; in short this thesis coined such a system "deformation-flow" system. The infrastructure here refers to the network of channels. This thesis is built upon the work of (Mosadegh et al., 2010), however presenting a new idea for one of the IMC components, switch valve, differently from the work of (Mosadegh et al., 2010). The specific objectives are re-visited herein:

- ***Objective 1****: To investigate the new architecture of a micro-fluidic device that reduces the number of layers of flow-deformation systems for performing the function of switch valve.*
- ***Objective 2:*** *To develop an accurate simulation model for a flow-deformation system which is built upon the new architecture to predict the behavior of the system.*
- ***Objective 3****: To build a prototype for the foregoing flow-deformation system to prove that the proposed architecture works.*

Specifically, the new idea in Objective 1 is to change the orientation of multi-layers from the vertical direction to the horizontal direction, and as such the channels and membranes inside the channels may be fabricated once to avoid the challenge of assemble three pieces vertically, which is the case of the work of (Mosadegh et al., 2010). This idea may be called “horizontal stacking”.

Overall, this thesis has proved that the idea of horizontal stacking is feasible through the systematic and rational design of the device based on the idea (in Chapter 3), simulation in Chapter 4, fabrication (in Chapter 5), and testing (in Chapter 6). Specifically, the ADT (axiomatic design theory), especially its first axiom, was applied to guide the design process. The material to build the device is PDMS owing to its proven biocompatibility and high elasticity. The simulation of the behavior of the device was carried out by the multi-phase physics software called COMSOL. It is worth to mention that the simulation has verified the design. Both the hard and soft lithography methods were combined to fabricate the device. A limited testing was performed owning to the restriction of the measurement instrument as well as the restriction of adequate fabrication facility available to this research.

The main conclusions drawn from the work on this thesis are: (1) the principle of horizontal stacking to build an IMC switch valve is feasible, (2) the UV based lithography method for fabricating such a device is not suitable because of its limited capability of making the high aspect ratio feature of the device, and the deep X-ray based lithography method should be employed.

7.2 Contribution

The first contribution of this thesis is the proof-of-concept of the horizontal stacking of channels and membranes to build an IMC, switch valve in this case, in the field of micro-fluidic circuit. The current literature builds an IMC based on the idea of vertical stacking, which meets challenges in alignment of multi-layers in assembly.

The second contribution of this thesis is the generalization of the IMC system to a device principle called deformation-flow principle for the solid-fluid system, of which the micro-fluidic system is a kind. This principle says that a fluid device can be built based on the coupling of deformable solids and fluids in such a way that the deformation of solids changes the flow behavior while the flow of fluids changes the deformation behavior.

The third contribution of this thesis is the concept of generalized switch valve, i.e., the switch valve is not just with the on-or-off mode but the mode of the x percent and y percent with $x + y = 100$. This concept of fluid devices may be called a continuous switch valve. This device concept may add value to IMC systems in that it is in line with the analogous nature of fluids, which may have implication to building a more sophisticate IMC systems in future. A care needs to be taken, however, that this concept has only been indirectly proved with the simulation facility.

7.3 Limitations

There are several limitations with this work. The first limitation is the restriction of the fabrication facility available to build the device, especially the high aspect ratio lithography facility. The desired thickness of the membrane, 5 μm, turns out to be impossibly made with the fabrication facility available. The second limitation is the restriction of the measurement tool available. The current measurement tool has the resolution of 5.9 μm only, which is too large to measure the deflection of 0.05 μm in order to verify the simulation result. This restriction also causes the channel be not high enough (the Z-axis with respect to Figure 4.1), and this further causes the glass cover sticks on the bottom of the channel so that the fluid has difficulty to flow in the channel. This problem has made unable to measure the flow velocity quantitatively. There is also a limitation regarding the simulation tool. The computing facility is not enough to run the simulation of the entire system; only a part of the system (i.e., one membrane) is simulated. Fortunately, due to the symmetrical nature of the entire device, the simulation of the part of the system does not compromise the result.

7.4 Future work

Several recommendations for future work are made. First, the deep X-ray lithography should be employed to fabricate the membrane and channel, and dramatic reduction of the thickness of the membrane along with the increased height of the channel is expected. Second, fabrication of the membrane may be separated from fabrication of the channel, and after that, assembly of the membrane into the channel is made. Third, the membrane may be made much longer in the X-axis

(Figure 4.1) than the one made in this thesis to increase the flexibility of the membrane. Finally, new materials other than PDMS, which are more elastic, may need to be explored to improve the deformability of the membrane.

References

Adam, T., An, F., An, G., An, Q., Anfimov, N., Antonelli, V., … Zou, J. (2015). JUNO Conceptual Design Report. Retrieved from http://arxiv.org/abs/1508.07166

Chueh, B. H., Huh, D., Kyrtsos, C. R., Houssin, T., Futai, N., & Takayama, S. (2007). Leakage-free bonding of porous membranes into layered microfluidic array systems. *Analytical Chemistry*, *79*(9), 3504–3508. https://doi.org/10.1021/ac062118p

COMSOL Report. (n.d.).

Groisman, A. (2003). Microfluidic Memory and Control Devices. *Science*, *300*(5621), 955–958. https://doi.org/10.1126/science.1083694

Heidelberg Instruments DWL 66+. (n.d.).

Henning, A. K. (2007). Concepts for Micro-Pneumatic and Micro-Hydraulic Logic Gates. *MOEMS-MEMS 2007 Micro and Nanofabrication*, 64650T–64650T–12. https://doi.org/10.1117/12.697807

Jeon, N. L., Chiu, D. T., Wargo, C. J., Wu, H., Choi, I. S., Anderson, J. R., & Whitesides, G. M. (2002). Micro ¯ uidics Section : Design and Fabrication of Integrated Passive Valves and Pumps for Flexible Polymer 3-Dimensional Micro ¯ uidic Systems. *Biomedical Microdevices*, 117–121.

Kartalov, E. P., Walker, C., Taylor, C. R., Anderson, W. F., & Scherer, A. (2006). Microfluidic vias enable nested bioarrays and autoregulatory devices in Newtonian fluids. *Proceedings of the National Academy of Sciences of the United States of America*, *103*(33), 12280–4. https://doi.org/10.1073/pnas.0602890103

Langelier, S. M., Chang, D. S., Zeitoun, R. I., & Burns, M. a. (2009). Acoustically driven

programmable liquid motion using resonance cavities. *Proceedings of the National Academy of Sciences of the United States of America*, *106*(31), 12617–12622. https://doi.org/10.1073/pnas.0900043106

Liu, J., Chen, Y., Taylor, C. R., Scherer, A., & Kartalov, E. P. (2009). Elastomeric microfluidic diode and rectifier work with Newtonian fluids. *Journal of Applied Physics*, *106*(11). https://doi.org/10.1063/1.3268463

Mosadegh, B., Bersano-Begey, T., Park, J. Y., Burns, M. a, & Takayama, S. (2011). Next-generation integrated microfluidic circuits. *Lab on a Chip*, *11*(17), 2813–2818. https://doi.org/10.1039/c1lc20387h

Mosadegh, B., Kuo, C. H., Tung, Y. C., Torisawa, Y. S., Bersano-Begey, T., Tavana, H., & Takayama, S. (2010). Integrated elastomeric components for autonomous regulation of sequential and oscillatory flow switching in microfluidic devices. *Nature Physics*, *6*(6), 433–437. https://doi.org/10.1038/nphys1637

Pahl, G., Beitz, W., Blessing, L., Feldhusen, J., Grote, K.-H. H., & Wallace, K. (2013). *Engineering Design: A Systematic Approach* (Vol. 11). Springer Science & Business Media. https://doi.org/10.1049/sqj.1963.0055

Rus, D., & Tolley, M. T. (2015). Design, fabrication and control of soft robots. *Nature*, *521*(7553), 467–475. https://doi.org/10.1038/nature14543

Sheet, P. D. (n.d.). SUEX Epoxy Thick Film Sheets (TDFS) Preliminary Data Sheet SUEX Epoxy Thick Film Sheets (TDFS) Preliminary Data Sheet.

Sun, Z., Yang, G. S., Zhang, B., & Zhang, W. (2011). On the concept of the resilient machine. In *Industrial Electronics and Applications (ICIEA), 2011 6th IEEE Conference on* (pp. 357–360). IEEE.

Tu, Y. L., Zhang, W. J., Liu, X., Li, W., Chai, C.-L., & Deters, R. (2008). A disaster response management system based on the control systems technology. *International Journal of Critical Infrastructures*, *4*(3), 274–295. https://doi.org/10.1504/IJCIS.2008.017441

Wang, J. W., Wang, H. F., Zhang, W. J., Ip, W. H., & Furuta, K. (2014). *On a unified definition of the service system: What is its identity? IEEE Systems Journal* (Vol. 8). https://doi.org/10.1109/JSYST.2013.2260623

Wehner, M., Truby, R. L., Fitzgerald, D. J., Mosadegh, B., Whitesides, G. M., Lewis, J. A., & Wood, R. J. (2016). An integrated design and fabrication strategy for entirely soft, autonomous robots. *Nature*, *536*(7617), 451–455. https://doi.org/10.1038/nature19100

Yu, Y. S., & Zhao, Y. P. (2009). Deformation of PDMS membrane and microcantilever by a water droplet: Comparison between Mooney-Rivlin and linear elastic constitutive models. *Journal of Colloid and Interface Science*, *332*(2), 467–476. https://doi.org/10.1016/j.jcis.2008.12.054

Zhang, W. J. (2017). Lecture note- system and system design. Retrieved from http://www.engr.usask.ca/classes/ME/886/

Zhang, W. J., & van Luttervelt, C. A. (2011). Toward a resilient manufacturing system. *CIRP Annals*, *60*(1), 469–472. https://doi.org/10.1016/J.CIRP.2011.03.041

Appendix A: Engineering drawings of the prototype system

This section is related to the drawing of the new switch valve and the new membrane specification including dimensions that have been used for fabricating the device.

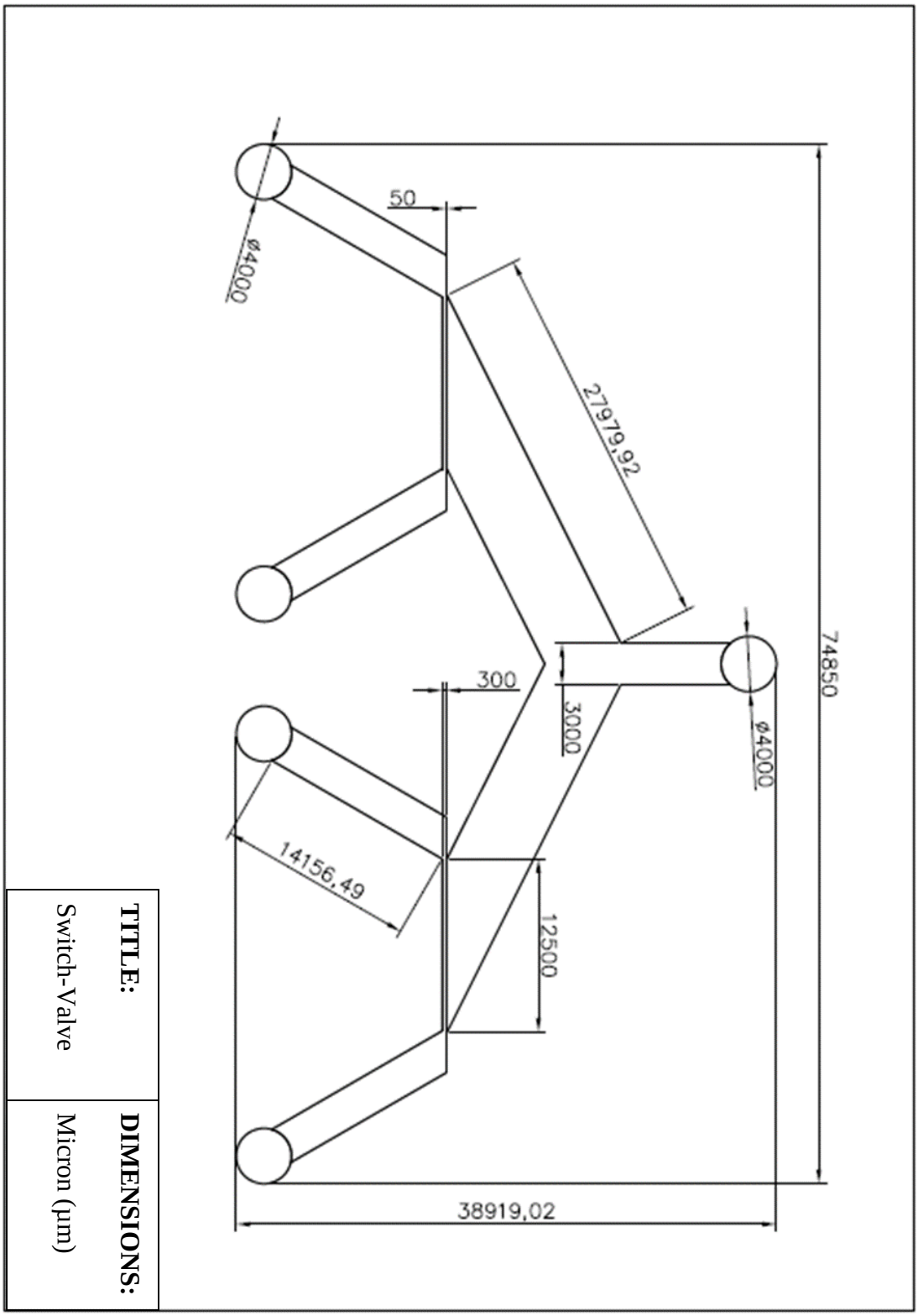

Figure A.1 The exact Dimension of the Switch Valve in micron (µm)

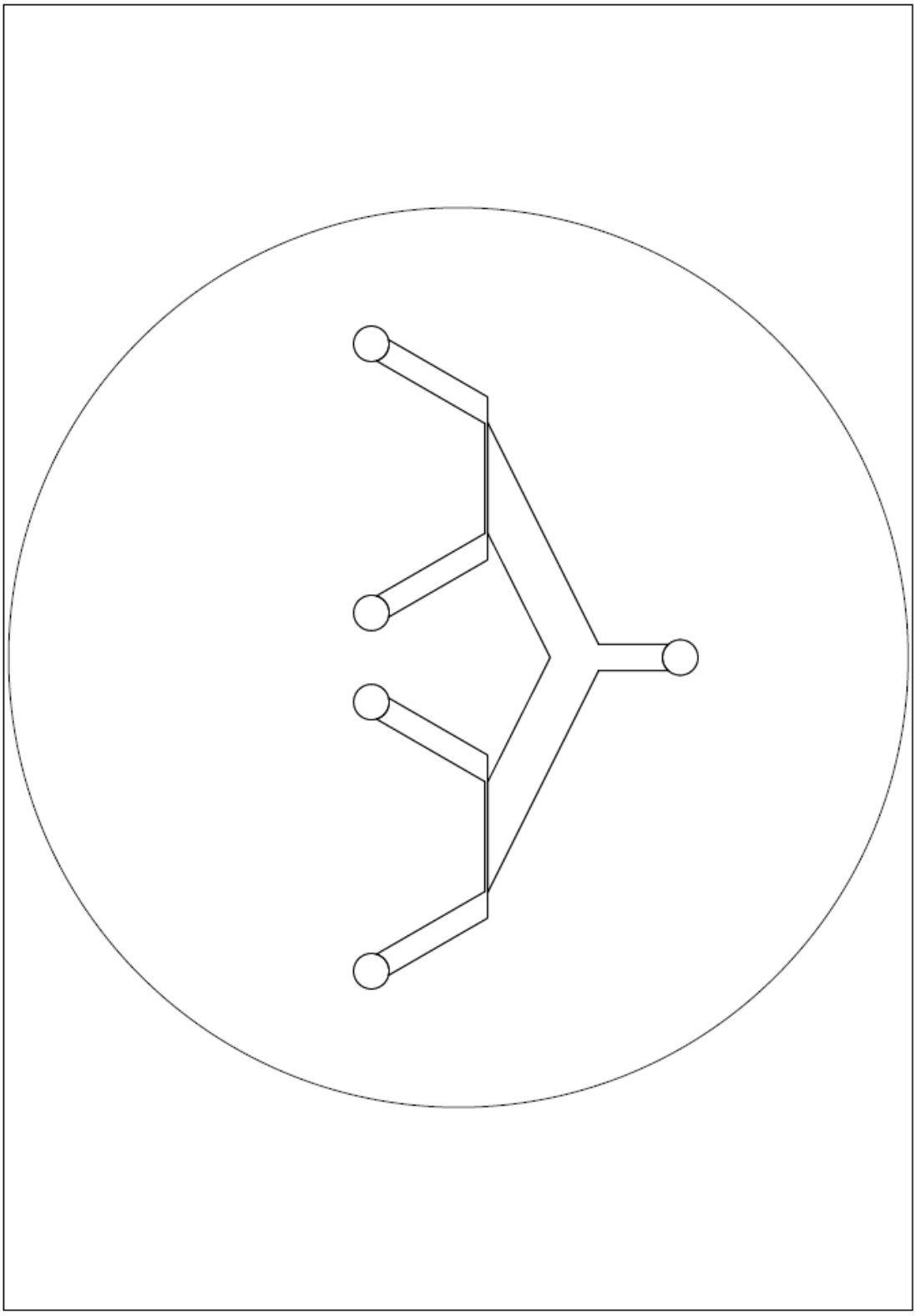

Figure A.2 The proposed design of the Switch Valve on top of a Silicon Wafer

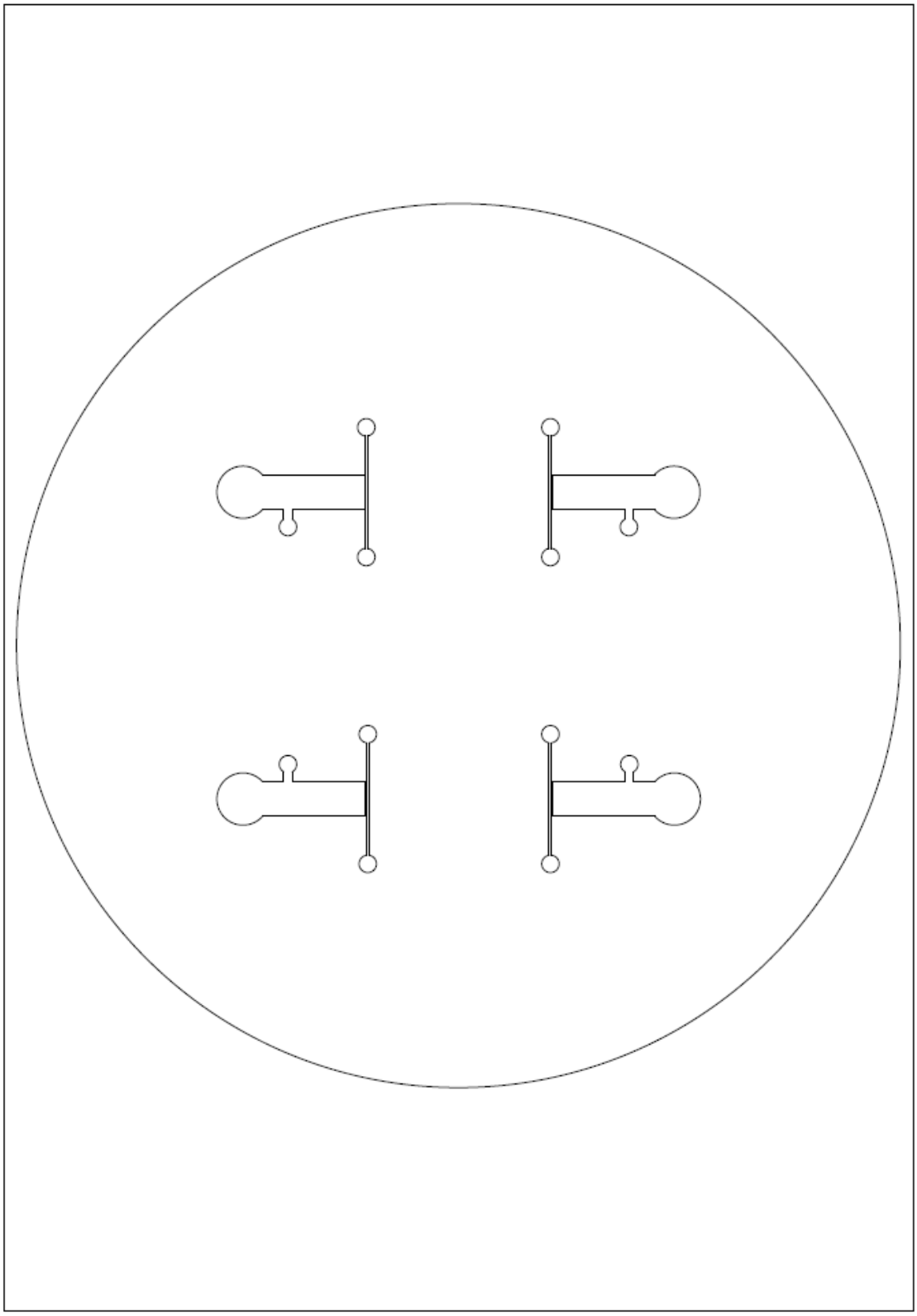

Figure A.3 Four membranes in one Silicon Wafer

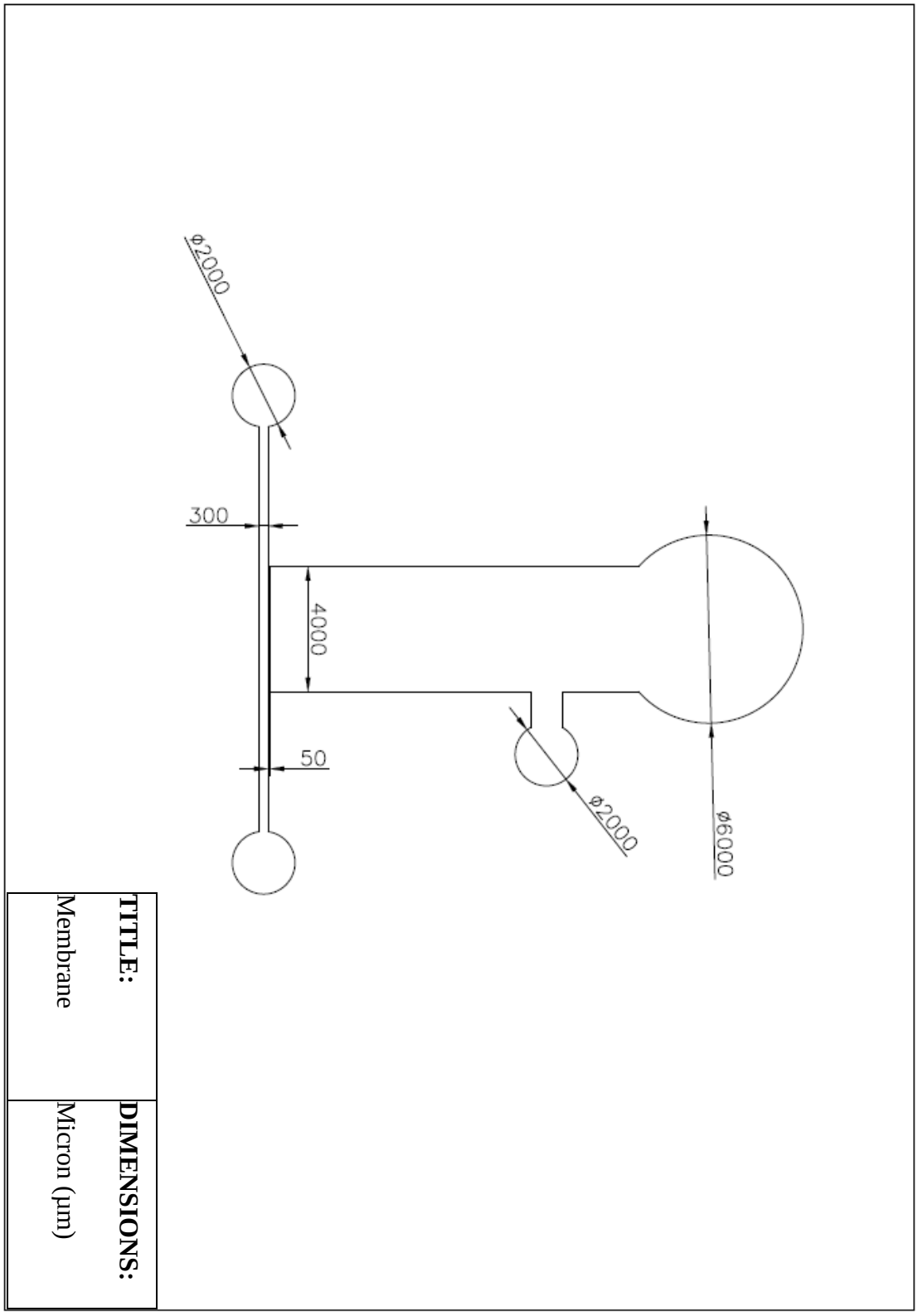

Figure A.4 The exact Dimension of one of Membrane with the thickness of 50µm

Appendix B: Permission to reproduce Content

SPRINGER NATURE LICENSE
TERMS AND CONDITIONS

Oct 01, 2018

This Agreement between University of Saskatchewan -- Ashkan Rasouli ("You") and Springer Nature ("Springer Nature") consists of your license details and the terms and conditions provided by Springer Nature and Copyright Clearance Center.

License Number	4440330989998
License date	Oct 01, 2018
Licensed Content Publisher	Springer Nature
Licensed Content Publication	Nature Physics
Licensed Content Title	Integrated elastomeric components for autonomous regulation of sequential and oscillatory flow switching in microfluidic devices
Licensed Content Author	Bobak Mosadegh, Chuan-Hsien Kuo, Yi-Chung Tung, Yu-suke Torisawa, Tommaso Bersano-Begey et al.
Licensed Content Date	Apr 18, 2010
Licensed Content Volume	6
Licensed Content Issue	6
Type of Use	Thesis/Dissertation
Requestor type	academic/university or research institute
Format	print and electronic
Portion	figures/tables/illustrations
Number of figures/tables /illustrations	2
High-res required	no
Will you be translating?	no
Circulation/distribution	<501
Author of this Springer Nature content	no
Title	DESIGN OF A NEW MICROFLUIDIC SWITCH VALVE WITH EMBEDDED INSTRUCTIONS
Instructor name	Dr.Chris Zhang
Institution name	University of Saskatchewan
Expected presentation date	Dec 2018
Portions	Figure 1 and Figure 2
Requestor Location	University of Saskatchewan 69 Campus Drive Saskatoon, SK S7N 5B1 Canada Attn: Ashkan Rasouli
Billing Type	Invoice

Billing Address	University of Saskatchewan 69 Campus Drive Saskatoon, SK S7N 5B1 Canada Attn: Ashkan Rasouli
Total	0.00 CAD

SPRINGER NATURE LICENSE
TERMS AND CONDITIONS

Oct 02, 2018

This Agreement between University of Saskatchewan -- Ashkan Rasouli ("You") and Springer Nature ("Springer Nature") consists of your license details and the terms and conditions provided by Springer Nature and Copyright Clearance Center.

License Number	4440921140758
License date	Oct 02, 2018
Licensed Content Publisher	Springer Nature
Licensed Content Publication	Nature
Licensed Content Title	An integrated design and fabrication strategy for entirely soft, autonomous robots
Licensed Content Author	Michael Wehner, Ryan L. Truby, Daniel J. Fitzgerald, Bobak Mosadegh, George M. Whitesides et al.
Licensed Content Date	Aug 24, 2016
Licensed Content Volume	536
Licensed Content Issue	7617
Type of Use	Thesis/Dissertation
Requestor type	academic/university or research institute
Format	print and electronic
Portion	figures/tables/illustrations
Number of figures/tables /illustrations	1
High-res required	no
Will you be translating?	no
Circulation/distribution	<501
Author of this Springer Nature content	no
Title	DESIGN OF A NEW MICROFLUIDIC SWITCH VALVE WITH EMBEDDED INSTRUCTIONS
Instructor name	Dr.Chris Zhang
Institution name	University of Saskatchewan
Expected presentation date	Dec 2018
Portions	Figure 3
Requestor Location	University of Saskatchewan 69 Campus Drive Saskatoon, SK S7N 5B1 Canada Attn: Ashkan Rasouli
Billing Type	Invoice

Billing Address	University of Saskatchewan 69 Campus Drive Saskatoon, SK S7N 5B1 Canada Attn: Ashkan Rasouli
Total	0.00 CAD

Copyright Clearance Center

Note: Copyright.com supplies permissions but not the copyrighted content itself.

1 PAYMENT | 2 REVIEW | **3 CONFIRMATION**

Step 3: Order Confirmation

Thank you for your order! A confirmation for your order will be sent to your account email address. If you have questions about your order, you can call us 24 hrs/day, M-F at +1.855.239.3415 Toll Free, or write to us at info@copyright.com. This is not an invoice.

Confirmation Number: 11753304
Order Date: 10/02/2018

If you paid by credit card, your order will be finalized and your card will be charged within 24 hours. If you choose to be invoiced, you can change or cancel your order until the invoice is generated.

Payment Information

Ashkan Rasouli
University of Saskatchewan
asr661@mail.usask.ca
+1 (306) 966-5440
Payment Method: n/a

Order Details

Lab on a chip

Order detail ID:	71586769
Order License Id:	4440930691658
ISSN:	1473-0189
Publication Type:	e-Journal
Volume:	
Issue:	
Start page:	
Publisher:	ROYAL SOCIETY OF CHEMISTRY
Author/Editor:	Royal Society of Chemistry (Great Britain)

Permission Status: Granted
Permission type: Republish or display content
Type of use: Thesis/Dissertation
View details

Note: This item will be invoiced or charged separately through CCC's **RightsLink** service. More info **$ 0.00**

Total order items: 1

This is not an invoice.

Order Total: 0.00 USD

Appendix C: Calibration and Uncertainty measurement

C.1 Uncertainty in measurement

Systematic uncertainty

The systematic uncertainty is mostly related to instrumental accuracy. For this study the calibration that has been done has accuracy of 5.9 µm per pixel which means that any measurement below this amount cannot be gained. Therefore, for this study this amount would be given as systematic uncertainty.

Total uncertainty

The total amount of uncertainty is based on the two different uncertainty. In other words, it is equal to systematic and random uncertainty. Also, the random uncertainty in this study also stated as standard error which can be calculated by having the standard deviation of the experimental results. That is to divide the standard deviation by the square root if number of experiments. Therefore, the total uncertainty would be calculated based on the equation (C.1).

$$U_t = \sqrt{u_r^2 + u_S^2} \qquad \text{(C.1)}$$

where u_r and u_s would be the random and systematic uncertainty, respectively.

Based on Table 4.1 for the random uncertainty, we have 1.68µm. therefore, for the final result for total uncertainty, 6.09µm can be calculated based on the equation (C.1)

C.2 Calibration

The calibration has been done using the multifunction target calibrator as it can be seen on figure C.1. By using this calibrator, the microscope which can be seen on figure C.3 is calibrated and then based on the calibration results, the exact amount of deflection can be measured. Also, as it can be seen on figure C.2, the calibrator bar is burned inside the figure and can be used for future studies where with any kind of image calibration software such as ImageJ, the same measurement can be acquired.

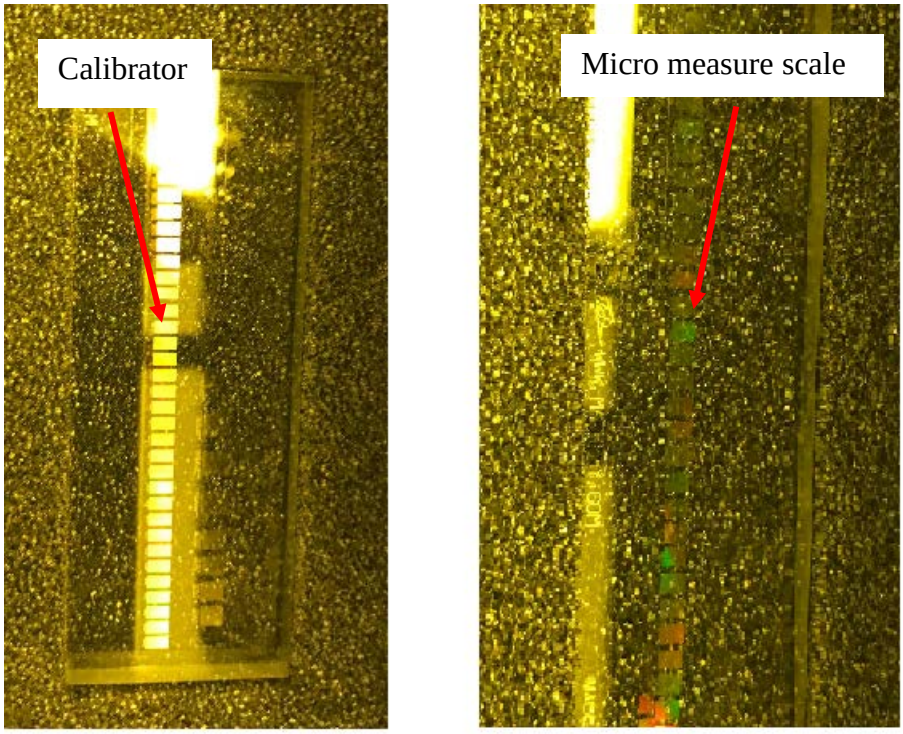

Figure C.1 Multifunction target calibrator (Model DA030). It has a precise measurement which can be viewed under the microscope and with that precise measurements the calibration can be done.

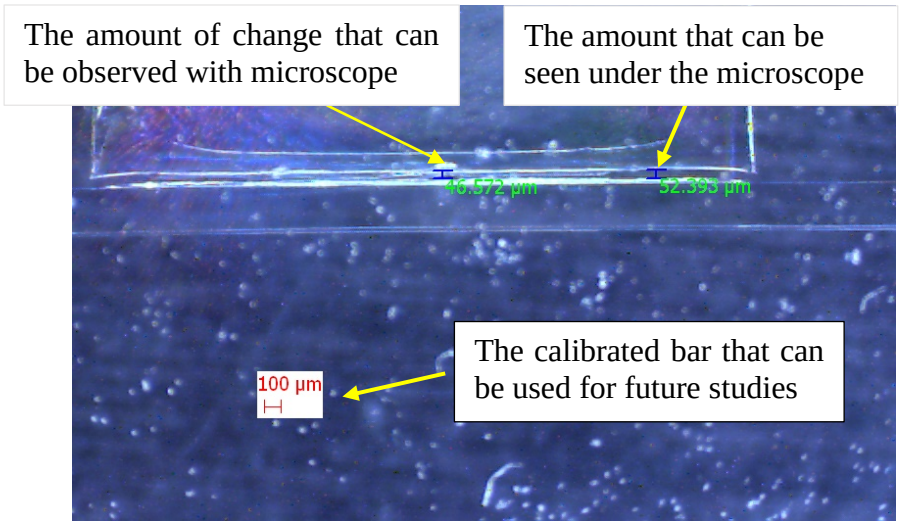

Figure C.2 The measurements which have been done by using a microscope

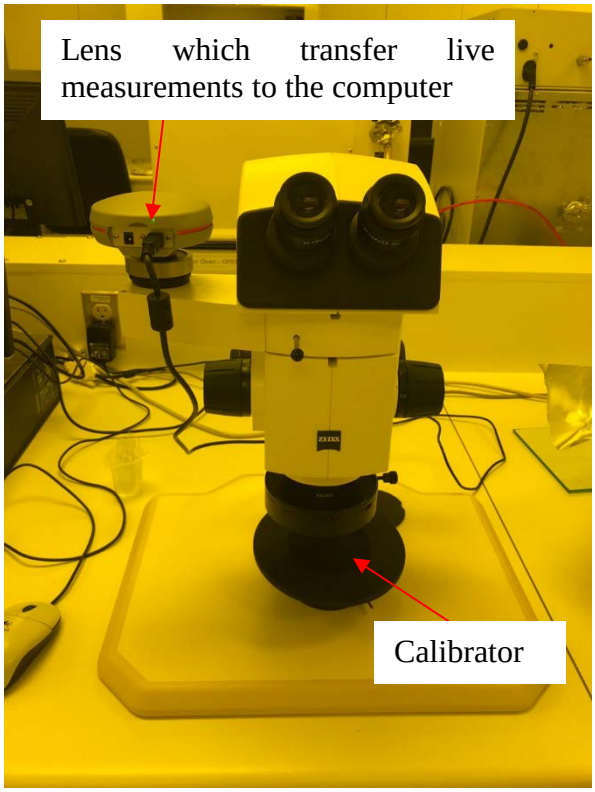

Figure C.3 Microscope which used for capturing some of the images and also measure the calibration